J. Fluid Mech. (1981), *vol.* 107, *pp.* 297–338
Printed in Great Britain

New aspects of turbulent boundary-layer structure

By M. R. HEAD AND P. BANDYOPADHYAY
Department of Engineering, University of Cambridge

(Received 27 July 1979 and in revised form 7 September 1980)

Flow visualization studies of the zero-pressure-gradient turbulent boundary layer over the Reynolds-number range $500 < Re_\theta < 17500$ have shown large Reynolds-number effects on boundary-layer structure.

At high Reynolds numbers ($Re_\theta > 2000$, say) the layer appears to consist very largely of elongated hairpin vortices or vortex pairs, originating in the wall region and extending through a large part of the boundary-layer thickness or beyond it; they are for the most part inclined to the wall at a characteristic angle in the region of 40–50°. Large-scale features, which exhibit a slow overturning motion, appear to consist mainly of random arrays of such hairpin vortices, although there is some evidence of more systematic structures.

At low Reynolds numbers ($Re_\theta < 800$, say) the hairpin vortices are very much less elongated and are better described as horseshoe vortices or vortex loops; large-scale features now consist simply of isolated vortex loops (at the very lowest Reynolds numbers), or of several such loops interacting strongly, and show a relatively brisk rate of rotation.

1. Introduction

The object of this paper is to present a picture of turbulent boundary-layer structure that appears to differ rather widely from generally accepted ideas, although it matches the observations of other authors at several crucial points. It has emerged from a series of experiments in which both flow-visualization and hot-wire techniques have been used, and it is doubtful whether, in the present hands at least, either technique used by itself would have led to a satisfactory conclusion.

The essential feature of the picture presented here is the existence of large numbers of vortex pairs, or hairpin vortices, extending through at least a substantial part of the boundary-layer thickness, and inclined at a more or less constant characteristic angle to the surface. These vortex pairs may be (and very often are) greatly distorted, and at high Reynolds numbers may be enormously elongated, but they remain identifiable in the ciné films we have made, and in the selected frames shown here.

A good deal of what follows has already been presented by the authors (Bandyopadhyay 1977; Head & Bandyopadhyay 1978) and it will, of course, be recognized that the picture has much in common with the earlier proposals of Theodorsen (1952) and Black (1966, 1968). These earlier proposals, however, tended to be rather in the nature of intuitively appealing hypotheses, supported only indirectly by experimental evidence, whereas the present picture is one which has, in effect, been forced upon the authors by the weight of the evidence that has accumulated in the course of the experiments described below. At the outset, nothing could have seemed more

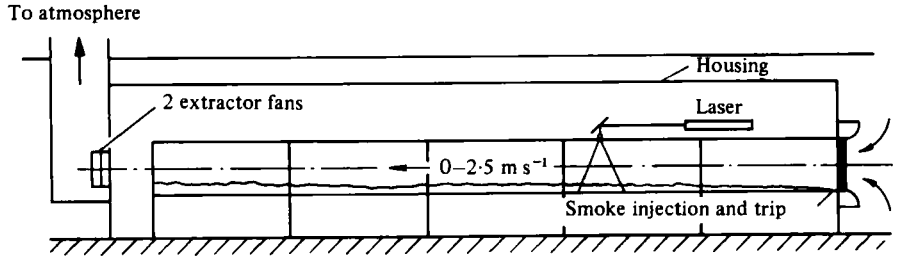

FIGURE 1. Low-speed smoke tunnel.

implausible than that the boundary layer should consist almost exclusively of vortex loops or hairpins originating in the wall region, with dimensions here scaling on wall variables, and that some at least of these same vortex loops or hairpins should extend right through the boundary layer even at high Reynolds numbers ($Re_\theta \simeq 10000$), but this is the conclusion we have now come to accept.

The seeming implausibility of the present picture may explain why it was not discovered earlier, but there are probably other contributory reasons. For a start, most investigations have been made using hot wires, and, while these are ideal for determining the statistical properties of turbulence, they are much less satisfactory for revealing the existence of organized flow structures that may vary widely in size and orientation. This, however, is just the information we might expect to obtain from flow-visualization studies, but here the trouble seems to have been that almost all investigators have used techniques which limit the observations to relatively low Reynolds numbers, where, as we shall see later, the structure is markedly different from that at high Reynolds numbers, with vortex lines tending to appear as low-aspect-ratio loops rather than extended vortex pairs or hairpins.

In the present flow-visualization experiments, the range of Reynolds numbers covered in reasonable detail was from $Re_\theta \simeq 500$ to $Re_\theta \simeq 10000$, and the effects of increasing Reynolds number were readily apparent, mainly in the increased stretching of what appeared at low Reynolds numbers as horseshoe vortices or vortex loops. It is because these become extremely elongated (or stretched) at high Reynolds numbers that they are referred to here as vortex pairs or hairpins, although for $Re_\theta > 5000$ (say) even the latter term ceases to be adequately descriptive.

In the remainder of the report we shall first give a brief description of the flow-visualization technique and the facilities available, and follow this with a chronological account of the experiments and the results obtained.

2. Flow-visualization technique

This is essentially a development of that described by Fiedler & Head (1966), where a section of the turbulent boundary layer, filled with smoke, is illuminated by an intense plane of light. A low-speed wind tunnel with a very long working section had been constructed in the laboratory some ten years ago to exploit this technique, and in its present form is shown in figure 1. Earlier it had been used by the first author to make a film which was shown at the Boeing Symposium on Turbulence (1969), and by Falco in his investigation of typical eddies (Falco 1974, 1977; Falco & Newman

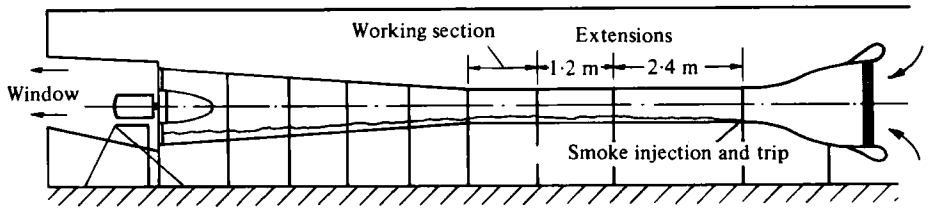

FIGURE 2. Adapted laboratory tunnel.

1974). For the present experiments the lighting system was improved by the use of a 4 W argon-ion laser for illumination, the beam being fanned out into a plane by the use of either a cylindrical lens or a glass rod with a diameter in the range 3–10 mm. This simple system had earlier been used by Fiedler (1970, private communication). For the later experiments a 5 W laser was used in place of the 4 W laser.

With this system of illumination, and the boundary layer filled with smoke produced by a smoke generator, it was possible to obtain satisfactory results up to framing rates of about 1500 per second and free-stream velocities in the region of 25 m s^{-1}. It was not possible to achieve such velocities in the smoke tunnel, and the high-Reynolds-number results ($Re_\theta > 2200$) were all obtained in another straight-through tunnel in the laboratory, modified by fitting an extension between the contraction and the normal working section. In the earlier experiments this extension was 2·4 m (8 ft) long and in the later experiments 3·6 m (12 ft) long. To keep the laboratory clear of smoke, the outlet from the tunnel was ducted to a nearby window. The general arrangement is shown in figure 2.

The main features of the arrangements just described have been incorporated in an improved smoke tunnel described by Falco (1978), and further details of the flow visualization technique may be obtained from that paper.

Photography was normally performed using a 16 mm Fastax camera with Ilford Mark V film, the effective ASA number of the film being substantially increased by the use of Microphen developer, with developing times up to 25 minutes. Flash photographs, and short exposure single shots using laser illumination, were also taken on 35 mm HP5 film using a Nikon F camera.

A frame-analysis projector, which could be stopped, reversed and run at different speeds, was used to examine the films.

3. Hot-wire measurements

With the use of smoke (i.e. condensed light-oil vapour) for flow visualization, simultaneous measurements can be made in the boundary layer using hot wires, so long as the overheat ratio is kept reasonably high (see, for example, Fiedler & Head 1966; Falco 1978). Falco & Newman (1974) had combined the flow visualization and hot-wire techniques by displaying the hot-wire signals on a storage oscilloscope which was photographed along with the illuminated section of the boundary layer, and this system was retained for the initial experiments described here, with the important modification that the hot-wire signals were also recorded on magnetic tape, along with a timing signal which actuated a counter within the field of view of the camera.

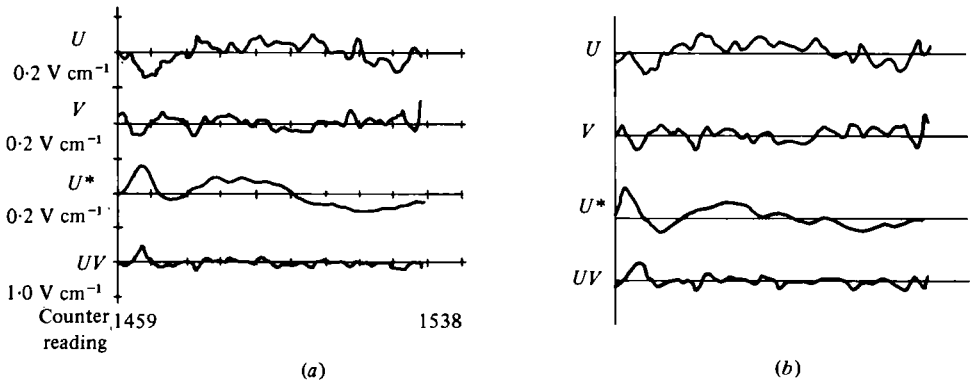

FIGURE 3. Comparison between (*a*) Calcomp plot and (*b*) oscilloscope record.

The data recorded on magnetic tape were digitized and stored on floppy disc, and could be processed and Calcomp plotted as required. The stored information included counts of the sine waves or square waves used for the timing signal, and these could be compared with the counter readings recorded on film to achieve synchronization. To check on the accuracy of synchronization and the taping procedure generally, the photographed oscilloscope traces could be compared with the Calcomp-plotted signals covering the same range of counter readings. With a transient-free start to the timing signal it was found that computer counts tied in accurately with photographed counter readings, and that the hot-wire signals obtained by photographing the oscilloscope were satisfactorily reproduced in the Calcomp plots of the digitized data recorded on tape. Figure 3 shows a typical comparison.

4. Preliminary experiments

Initial hot-wire and flow-visualization experiments were mainly confined to validating the procedure just described, a crossed wire positioned in the outer part of the layer giving values of u', v' and $u'v'$ there, while a single hot wire very close to the surface gave an indication of the instantaneous skin friction. Once the problem of synchronization had been solved, attention was given to the problem of presenting the information contained in the tape and on the film in a readily assimilable form, and in such a way that the two sets of information could be viewed simultaneously. This happened more or less automatically with the hot-wire signals displayed on the oscilloscope and photographed along with the illuminated section of the layer, and changes in u', v' and $u'v'$ could be readily associated with visually identifiable features. Figure 4, for example, shows the changes in these quantities occurring when a fairly well-defined interface is convected past the hot wires.

However, the situation is very different when the information is stored in digital form and output as a Calcomp plot. The timing-signal counts enable the plotted signals to be associated with corresponding frames of the film, but this is very different from having them displayed directly upon the screen as the film is run through the projector either continuously or frame by frame, and correspondences between visually identifiable flow features and the signals to which they give rise will be much more difficult to pick up.

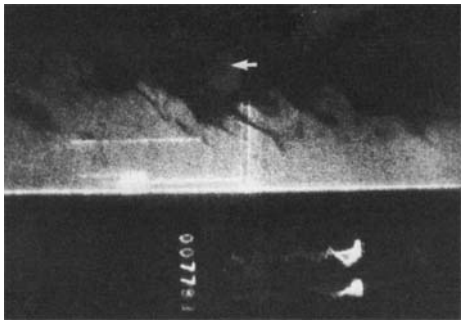

FIGURE 4. Simultaneous passage of interface past two hot wires.

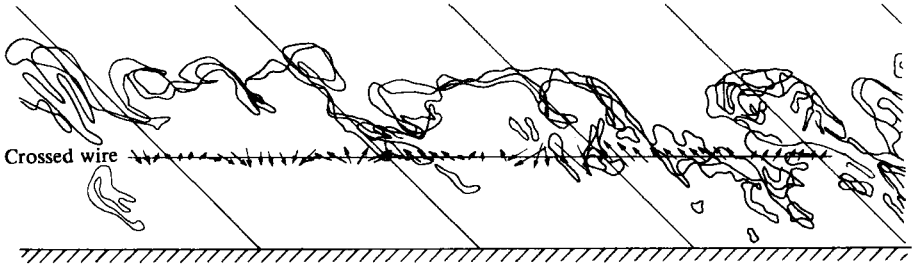

FIGURE 5. Vector plot of disturbance velocities with the edge of the smoke indicated.

A technique was tried which we shall briefly discuss. Although it did not prove immediately useful here, it may be worth bearing in mind for future application.

Over a limited sample length, digitized values of u' and v' obtained from the crossed-wire signal were processed at equal time intervals to give vectors representing the instantaneous disturbance velocity. These velocity vectors were then plotted to a suitable but arbitrary scale at equal intervals defined by $\overline{u}/t$, where $\overline{u}$ is the mean velocity at the level of the crossed wire and t is the time interval at which the vectors were determined.

Any one vector would have associated with it a particular timing-signal count, and the outline of the smoke-filled boundary layer corresponding to this count could be obtained by projecting the appropriate frame on to the paper and pencilling-in the edge of the smoke-filled region. This could have been done for each vector but would have produced a rather confused picture, and in fact the outline changed only relatively slowly as the features moved downstream, so that the outline was redrawn only for (say) every tenth vector, the outlines corresponding to different vectors being distinguished by different colours. Part of such a record is shown in figure 5. Because it is to a small scale and in monochrome it appears too confused to provide an adequate illustration of the technique, but it has been included, with lines at 45° to the surface superimposed, because it provided an early indication that such an angle might be of special significance in defining turbulent boundary-layer structure.

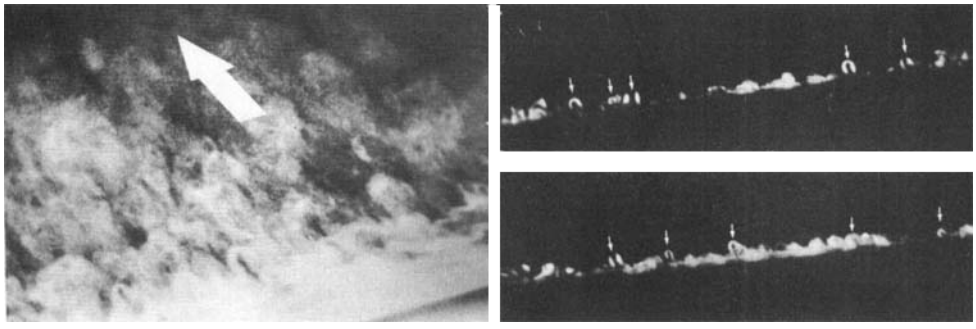

(*a*) (*b*)

FIGURE 6. Horseshoe vortices in reattaching flow behind circular rod. (*a*) General illumination, (*b*) illumination by transverse light plane.

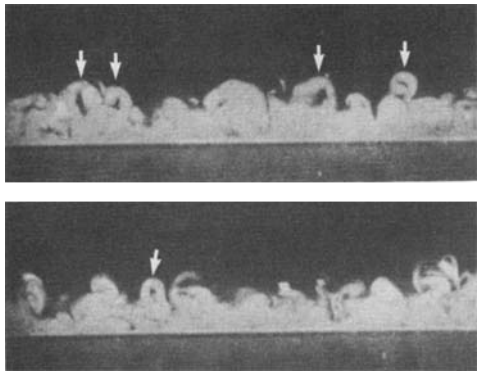

FIGURE 7. Horseshoe vortices in low-Reynolds-number boundary layer (cross-stream illumination, $Re_\theta \simeq 500$).

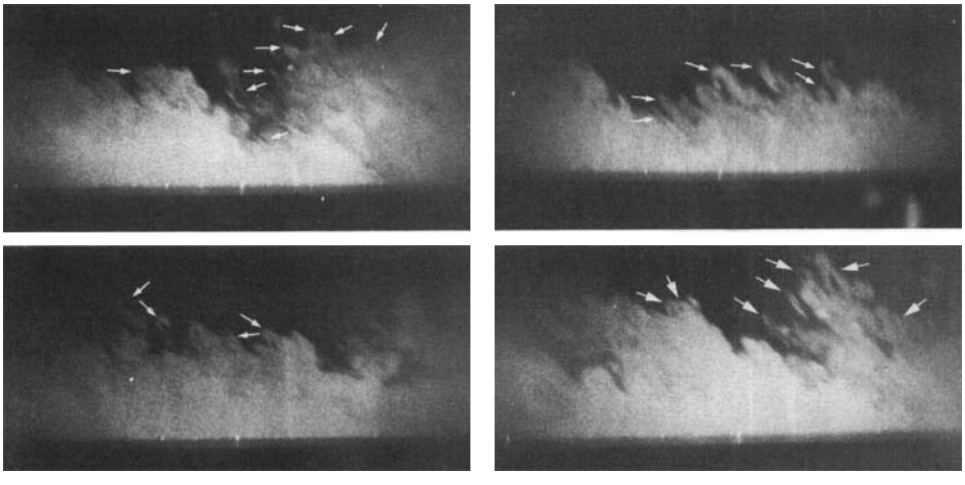

FIGURE 8. Examples of skewed hairpins or vortex loops.

5. Course of main investigation

5.1. *Experiments with hot wires and longitudinal light plane*

The preliminary experiments had shown no obvious correlation between the signals from the hot wire close to the surface and those from the crossed wire further out in the layer, but a close examination of the films and figures such as figure 5 suggested strongly that the edge of the layer at reasonably high Reynolds numbers ($Re_\theta > 1000$, say) was composed very largely of smoke-filled features and smoke-free fissures inclined at a characteristic angle to the surface which appeared to be in the region of 45°.

The visual evidence gave no grounds for expecting that this characteristic angle should extend into the sublayer where the wire closest to wall was situated in the preliminary experiments. This wire was therefore moved out to a y^+ of about 40 (for $Re_\theta \simeq 2000$), and the crossed wire was replaced by a second single wire, staggered behind the first so that the line joining the two wires made an angle of 40° to the surface; the outer wire was at rather more than half the boundary-layer thickness.

A ciné film was made in the large smoke tunnel (figure 1) with this hot-wire configuration, and this film, and the corresponding Calcomp-plotted hot-wire records, provided most of the material for the paper by Bandyopadhyay (1977). The Reynolds number for this film corresponded to $Re_\theta = 2200$. The most interesting feature of the results came from a visual examination of the signals from the two hot wires, which revealed quite extensive regions (up to about $2{\cdot}5\delta$ long) where the two signals were very similar indeed. If it were accepted that these similarities were not simply due to random coincidence, then they could only be explained by alternate strips of high- and low-velocity fluid being convected simultaneously past the two wires, and it was suggested that regular arrays of vortex pairs or hairpin vortices inclined at 40° to the surface would produce this result.

At this stage the suggestion was largely conjectural but it was given some credibility by the fact that vortex loops were a common feature of both the reattaching flow behind a circular rod used as a tripping device, and of cross-stream sections of the turbulent boundary layer at low Reynolds number. Details of these flows are shown in figures 6 and 7, where the loops or horseshoes in the latter are indicated by the arrows. They are evidently a very common feature of the layer.

There is also some evidence, from illuminated longitudinal sections, of their appearance at higher Reynolds numbers. First, there is the existence of 'islands' of smoke in the outer part of the flow, which is a feature one would expect if loops occasionally extended beyond the completely smoke-filled region, and, second, there is often direct visual evidence of the existence of loops which have evidently been skewed into the plane of illumination. Examples of these latter are shown in figure 8 with arrows indicating what appear to be skewed vortex loops. Whether or not they are accepted as such at this stage, the photographs certainly suggest the existence of large numbers of narrow features inclined at something like 45° to the wall.

Although there were grounds for believing that the observed similarities in the signals from the two wires might be due to arrays of hairpin vortices being swept past them, the possibility could not be ignored that the similarities might be quite due to chance (i.e. the chance coincidence of signals covering much the same frequency

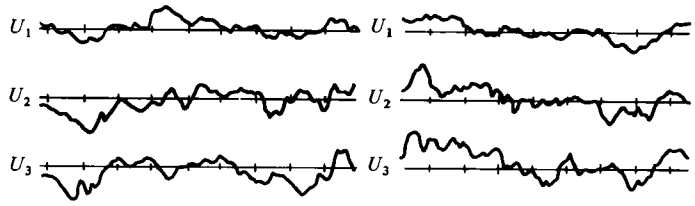

FIGURE 9. Typical signals from three wires showing limited similarity.

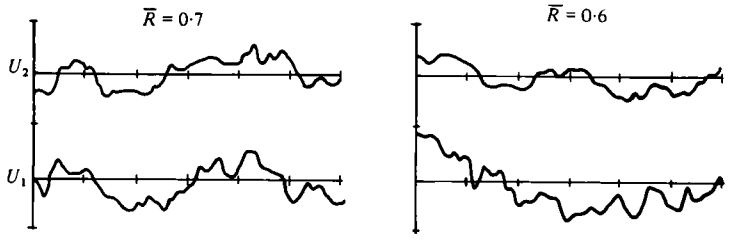

FIGURE 10. Examples of similar patches identified by computer.

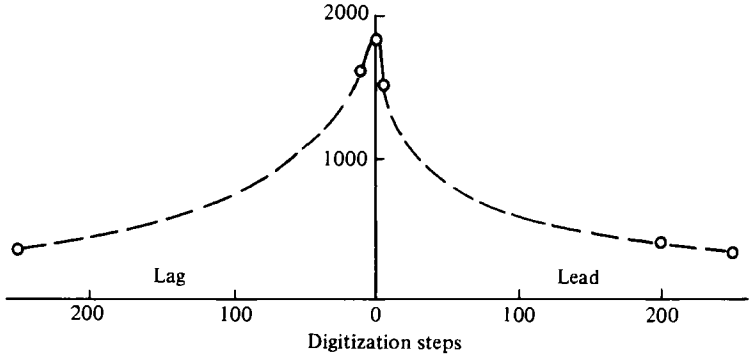

FIGURE 11. Effect of large lead or lag on the occurrence of similar patches. $\Sigma\overline{R}_{12}$ for $\overline{R}_{12} > 0{\cdot}7$, ciné 34A.

range). This possibility was effectively ruled out in two ways. First by inserting a third wire between the other two, and noting that the signals from two adjacent wires were more often similar than signals from the two most widely separated wires; and further that, where the signals from the two most widely separated wires were similar, the signals from adjacent wires were also similar. Figure 9 shows some typical results for $Re_\theta \simeq 2000$ obtained from Calcomp plots.

These results appeared fairly convincing but a further check was applied when a computer program was developed to detect regions of high correlation between two digitized signals. Typically, the program could be used to determine the total number of occasions, over a given sample length, on which the mean correlation over a distance of 2δ exceeded some stipulated value (say 0·7). Examples of similar patches identified by computer are shown in figure 10.

The program could be used with arbitrarily large lead or lag applied to one of the digitized signals, and if the similar patches had been due to random coincidence the results should have remained unaffected. In fact, however, as indicated in figure 11, large values of lead or lag resulted in a very marked reduction in the number of occasions on which the criterion $\bar{R} = 0{\cdot}7$ was exceeded.

It was thus demonstrated that the occurrence of similar patches was not due to random coincidence, and it seemed reasonable to conclude that they must be due to organized flow structures, inclined at an angle of approximately 40° to the surface, being swept past the wires. A variety of flow structures could be envisaged which might extend over a large part of the boundary-layer thickness (jets erupting from the wall region, for example, or large-scale circulations) but there were the further requirements that the flow structures must satisfy: they must extend at a more or less fixed angle to the wall and they must be of relatively small streamwise extent; both the hot-wire records and the visual evidence had made this clear. The only flow structure that seemed to satisfy these requirements was the extended vortex loop or hairpin vortex, which also seemed attractive for the reasons discussed earlier.

At this stage, then, it seemed likely from the hot-wire records that regular arrays of hairpin vortices were occasionally being convected past the wires, and in an effort to fit this observation into what appeared to be the generally accepted picture it was initially conjectured that such regular arrays might represent an early stage in the formation of large-scale coherent motions as these appeared to be generally understood, but when the films for $Re_\theta = 2200$ and 7500 were run through, and examined and re-examined, two features became apparent that seemed to contradict this hypothesis.

First, there seemed to be no evidence of large-scale coherent motions, other than a slow toppling or overturning motion that became noticeable only when the film was run reasonably fast (i.e. at 16 or 24 frames s^{-1}) with a fairly long streamwise extent of the boundary layer visible; in general, large-scale structures appeared to be no more than random agglomerations of much narrower features inclined at something like 40–45° to the wall.

Second, there seemed to be nothing visually distinctive about the regions where high correlations had been observed between hot-wire signals with the wires staggered at 40°; nor, in fact, had there been anything distinctive about the signals themselves other than the close agreement between them.

These points could be accounted for, however, if it were assumed that the boundary layer was at all times very largely composed of hairpin vortices, but that only occasionally were these hairpins sufficiently straight and closely aligned with the plane of the wires to produce similar signals over a substantial streamwise distance.

On this interpretation, the significance of the observed similar patches in the hot-wire records was much diminished, but they had served to draw attention to the fact that, for at least part of the time, narrow elongated structures existed, extending out from near the wall and not simply confined to the outer region of the boundary layer as the visual observations alone might have suggested: at the same time, the visual observations had provided support for the idea that the elongated structures were, in fact, stretched vortex loops or hairpins, and had suggested that they were of more or less universal occurrence.

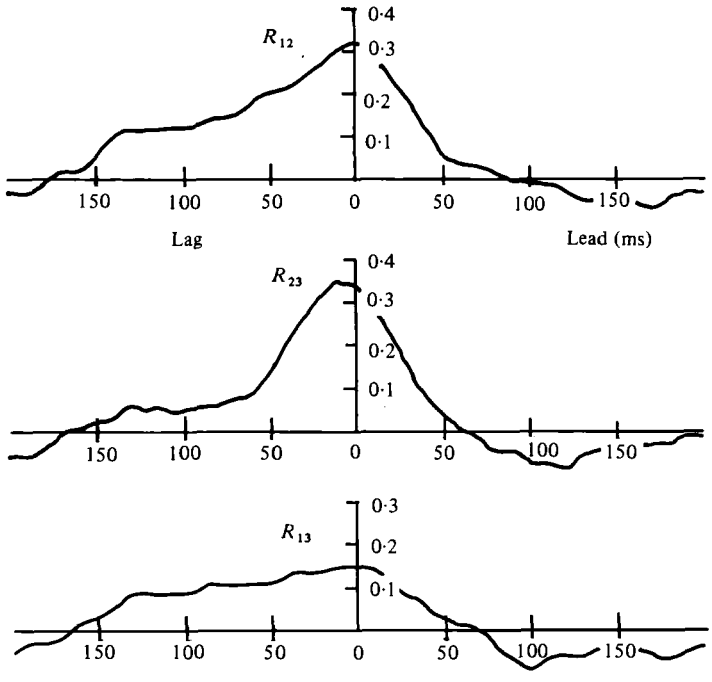

FIGURE 12. Effect of lead or lag on overall correlations.

Given that such hairpins (or stretched vortex loops, or vortex pairs) do exist, it would seem logical to suppose that they should remain active and distinct, and at the characteristic angle to the wall, for only a limited part of their lifetime, and that, at some stage, they should decay, rotate with the shear flow and form part of the smoke-filled background composing much of the flow. In a later section we shall discuss the possibilities in greater detail; here we shall go on to look at further hot-wire evidence for the existence of hairpin vortices inclined at something like 40° to the wall.

Before developing the computer program to distinguish regions of high correlation between two hot-wire signals, some of the digitized records were examined to determine the effect of small lead or lag on the overall correlation. A typical result with three staggered wires is shown in figure 12. With the wires numbered 1, 2 and 3 in order of their distance from the wall, we see, as would be expected, that the peak correlations between 1 and 2, and between 2 and 3 are much higher than that between 1 and 3. For 1 and 2, and 2 and 3, the peak correlation is somewhat greater than 0·3 and occurs for approximately zero lead or lag, indicating that the features giving rise to high correlation are inclined to the surface at the stagger angle of the wires (i.e. 40°). The correlations fall off rapidly with increasing lead (i.e. higher angles to the surface) but, particularly for the two wires closest to the wall, show a rather extended plateau-like region with increasing lag; the same feature will be seen in some of the results of Favre, Gaviglio & Dumas (1957).

The leads and lags shown in milliseconds in figure 12 may be converted into streamwise distances by assuming a mean convection velocity, and, with this taken as 0·75 of the free-stream velocity, the streamwise extent of the positive correlation turns out to be approximately 3δ. This is very much greater than would be accounted for

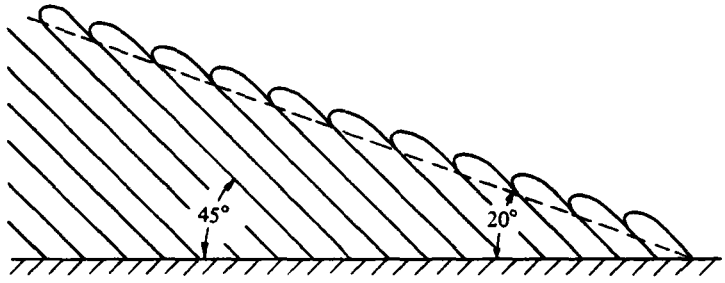

FIGURE 13. 20° interface formed by 45° features.

by the narrow features we have been considering, even with a considerable variation in their angles, and it would seem very likely that we are in fact observing the combined effects of two types of flow structure having very different scales, with narrow inclined features giving rise to the relatively high and sharp peaks for approximately zero lead or lag, and very much larger features producing longer-term variations from the mean. The relatively low correlation due to the large-scale features confirms what the films suggest, that there is little evidence of organized coherent large-scale motions at these Reynolds numbers.

Further evidence of two very different scales affecting the correlation was provided by results obtained with the computer program used to distinguish regions of high correlation. This is discussed fully in § 5 of the paper by Head & Bandyopadhyay (1978). Here we will only remark that, occasionally, high mean correlations between the signals from staggered hot wires were observed over streamwise distances of 2δ without any noticeable similarity of the small-scale fluctuations in the two signals. Where this occurred it was found to be due to the fact that the means of both signals over the length 2δ were appreciably different from the long-term means, both differing in the same sense. Thus there were a significant number of occasions on which velocity fluctuations occurred on scales of the order of δ (or multiples of δ) rather than small fractions of δ.

Returning now to the direct results of flow visualization, we should mention a feature that was occasionally observed in the ciné films, particularly at high Reynolds numbers. This was what appeared to be a series of narrow features (hairpins) inclined at the characteristic angle to the wall with their tips lying along a straight line which made a smaller angle to the wall, more or less as indicated in idealized form in the sketch (figure 13). Examples of such features are given in figure 14 (*a*, *b*), with lines at 20° to the surface indicated.

This result suggests very strongly that, at least occasionally, hairpins arise from the boundary in a regular sequence, with each hairpin as it leaves the surface giving rise to conditions that are favourable to the production of a further hairpin. Since the result of a vortex pair leaving the surface will be to induce a velocity between the limbs in an upstream direction, and thus a flow deceleration in the immediate vicinity of the wall, such a suggestion does not appear altogether implausible. What is rather odd is that such features should appear so rarely, at least at the present Reynolds numbers.

Before leaving this phase of the work, which was restricted to the use of longitudinal light planes (with and without hot wires) we should draw attention to figure 15 (*a*, *b*)

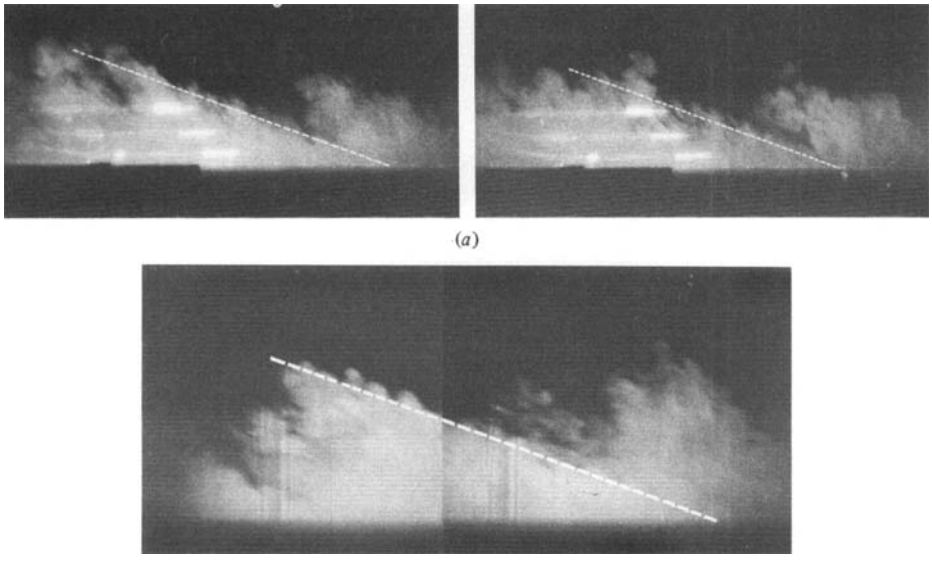

(*a*)

(*b*)

FIGURE 14. (*a*) Examples of features with interface inclined at approximately 20° to surface. (*b*) Example of 20° interface at $Re_\theta = 17500$ (this is a composite of two frames because of the restricted length of the light plane).

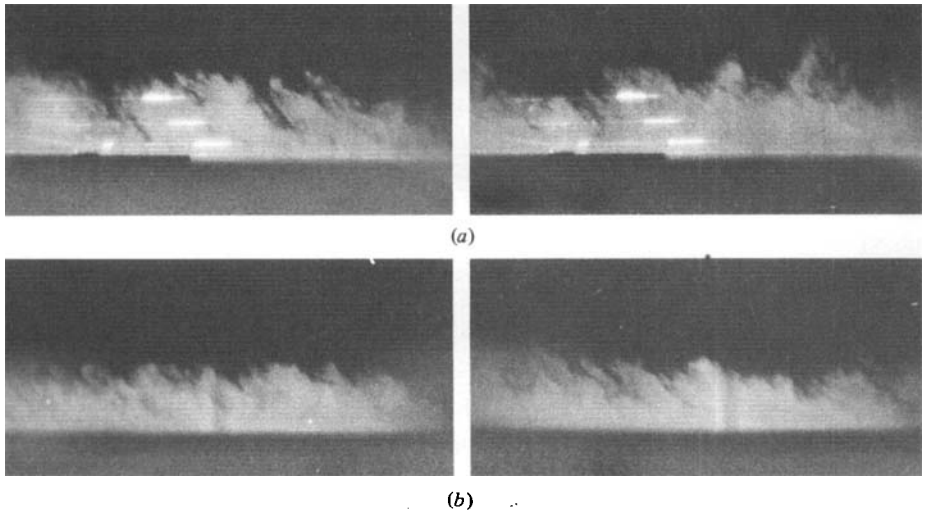

(*a*)

(*b*)

FIGURE 15. Boundary-layer structure at high Reynolds numbers. (*a*) $Re_\theta = 7500$; (*b*) $Re_\theta = 10500$.

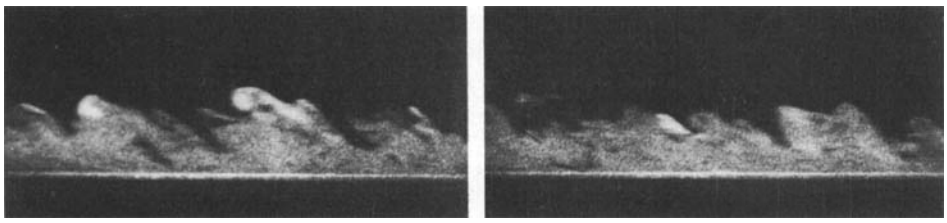

FIGURE 16. Boundary-layer structure at a low Reynolds number ($Re_\theta \simeq 500$; see also figure 34).

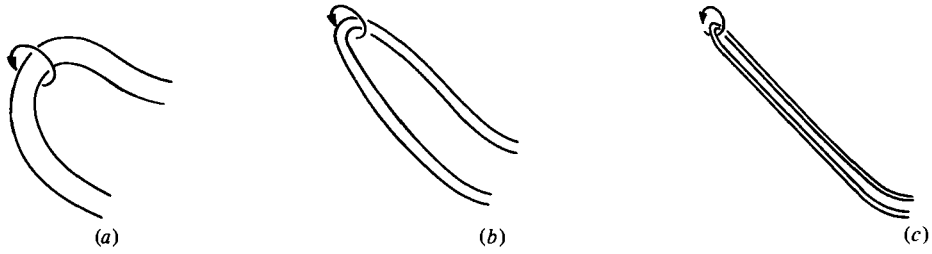

FIGURE 17. Effect of Reynolds number on features composing an outer region of turbulent boundary layer. (*a*) *Very* low *Re* (loops); (*b*) low–moderate *Re* (elongated loops or horseshoes); (*c*) moderate–high *Re* (elongated hairpins or vortex pairs).

which shows selected frames for two reasonably high Reynolds numbers ($Re_\theta = 7500$ and $Re_\theta = 10500$). This figure provides quite convincing evidence (we believe) of the predominance at these Reynolds numbers of long narrow structures inclined at something like 45° to the wall.

We may contrast this type of structure with that shown in figure 16 which is for a very much lower Reynolds number, probably in the range $Re_\theta = 400$–500. (The frames shown in this figure have been taken from the ciné film made for the 1969 Boeing Symposium and velocity profiles were not measured).

Comparing figures 15 and 16, and taking into account the results obtained at intermediate Reynolds numbers, we arrive at this stage at the hypothesis that the turbulent boundary layer is very largely composed at all Reynolds numbers (as least up to $Re_\theta \simeq 10000$) of vortex loops which have undergone very different degrees of stretching, as indicated in figure 17. This illustrates what we have termed the hairpin-vortex hypothesis and explains in a general way the distinction to be drawn between the terms 'vortex loop', 'horseshoe vortex' and 'hairpin vortex' or 'vortex pair' as used in the text.

5.2. *Flow visualization experiments with transverse light planes*

The work described above was completed towards the end of 1977 and at that time it seemed that the evidence in favour of the hairpin-vortex hypothesis was reasonably strong but by no means overwhelming. It was thought that experiments with a transverse inclined light plane should provide more decisive evidence, but the laser used for illumination, which had only been secured on loan, had meantime been restored to its owners. It was not until September 1978 that funds became available for the purchase of a replacement and films could be made with a transverse inclined light plane.

Here we should explain what such films might be expected to show on the basis of the hairpin-vortex hypothesis, with the vortices inclined to the wall at a characteristic angle in the region of 45°.

Let us consider one such vortex passing a light plane inclined (*a*) at an angle of 45° downstream and (*b*) at an angle of 45° upstream, as indicated in the sketch, figure 18.

With the light plane inclined downstream in the same direction as the hairpin, we should expect to see only a brief glimpse of the hairpin with the tip disappearing last as an isolated island if it is curled over into the flow as shown. With this inclination of the light plane we should expect vortex pairs to appear only relatively rarely, and for the most part the scene should be dominated by rapidly changing inverted

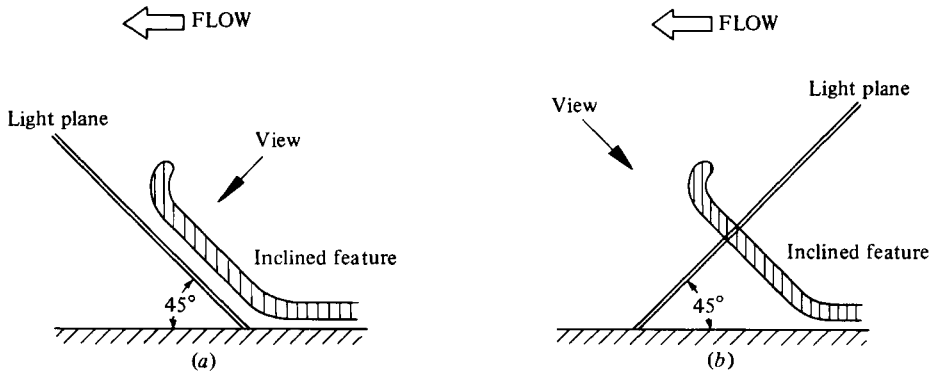

FIGURE 18. Inclined features being convected past light plane.
(*a*) Downstream light plane; (*b*) upstream light plane.

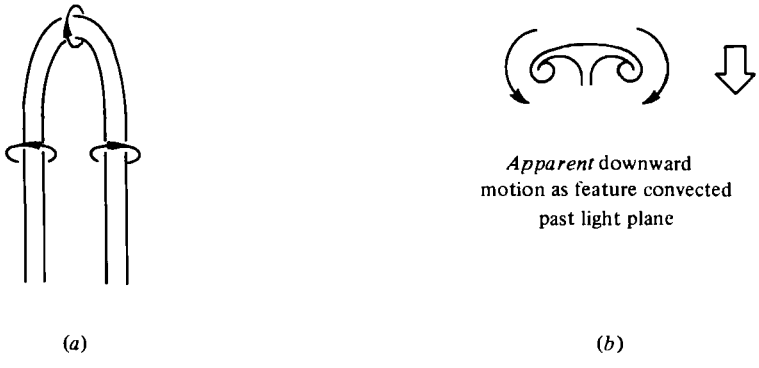

FIGURE 19. Views seen by camera as feature convected past light plane.
(*a*) 45° downstream light plane; (*b*) 45° upstream light plane.

U-shaped structures that become progressively more elongated as the Reynolds number increases.

On the other hand, with the light plane inclined at 45° *upstream* so that cross-sections of the hairpins are illuminated, we might expect to find that vortex pairs of different sizes and orientations should dominate the scene. As the hairpins are convected past the light plane, their cross-sections will appear to move towards the surface, and viewing the ciné film we should expect to see an apparent continuous motion towards the wall.

The contrast between the views with downstream and upstream light planes is shown in figure 19.

Of course the real situation is unlikely to be as simple and clear-cut as the sketches might suggest, and we must expect the real picture to be complicated by a variety of scales and by complex interactions between vortex pairs, particularly in the wall region.

All these expectations were fulfilled in the ciné films taken at the three Reynolds numbers Re_θ = 600, 1700 and 9400, with transverse light planes inclined upstream and downstream at 45°.

Figure 20 shows the experimental arrangement used in making the films. It was essentially the same in both tunnels, with illumination through a Perspex section in the floor and photography from above.

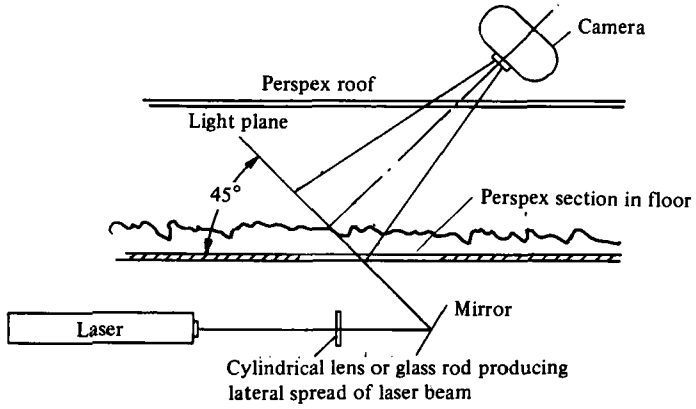

FIGURE 20. Experimental arrangement used with transverse inclined light planes.

Selected frames from the films are shown in figures 21(*a*, *b*), 22(*a*, *b*) and 23(*a*, *b*) where upstream and downstream views are compared at the three Reynolds numbers. It will of course be recognized that, while the frames are presented in pairs to emphasize the contrast between upstream and downstream views, the combinations are arbitrary and the pairs do not represent simultaneous photographs.

Two further points may be worth making. First, whilst the selection of only three frames from approximately 4000 would seem to provide scope for 'proving' almost anything, this would be true only if the flow were truly random; in fact the present choice of light planes reduces the degree of randomness enormously and the selected frames can be taken as quite reasonably representative both of the main features of the flows and of the general level of randomness that remains. The second point to be made is that the impressions gained from the ciné films are very much more vivid and convincing (we believe) than can be conveyed by the individual frames presented here (certainly for the films at $Re_\theta = 9400$), and the reader may be willing to bear this in mind.†

Comparing the views with downstream and upstream inclinations of the light plane, we note that they exhibit characteristic differences at all three Reynolds numbers. With the 45° downstream inclination the general appearance is that of continuous filaments with an overwhelming preponderance of extended loop-like structures. By contrast, the 45° upstream light plane shows the typically knotted type of structure we should expect, with cross-sections or the loop-like structures or hairpins appearing as vortex pairs. In the outer part of the layer these may be isolated, but over a considerable distance from the surface they appear sufficiently close for some measure of interference or mutual induction to be inevitable. Both views show the presence of a variety of scales, with the upstream light plane also showing a variety of orientations of the vortex pairs where these can be distinguished.

Comparing the results for different Reynolds numbers we see that there is a consistent reduction in the scales of the hairpins with increasing Re_θ. We also note that, at the two lower Reynolds numbers, the scales of the larger hairpins are also the dominant scales of the large-scale features, whereas at $Re_\theta = 9400$ the hairpins (which

† Copies of a short film are available from the authors.

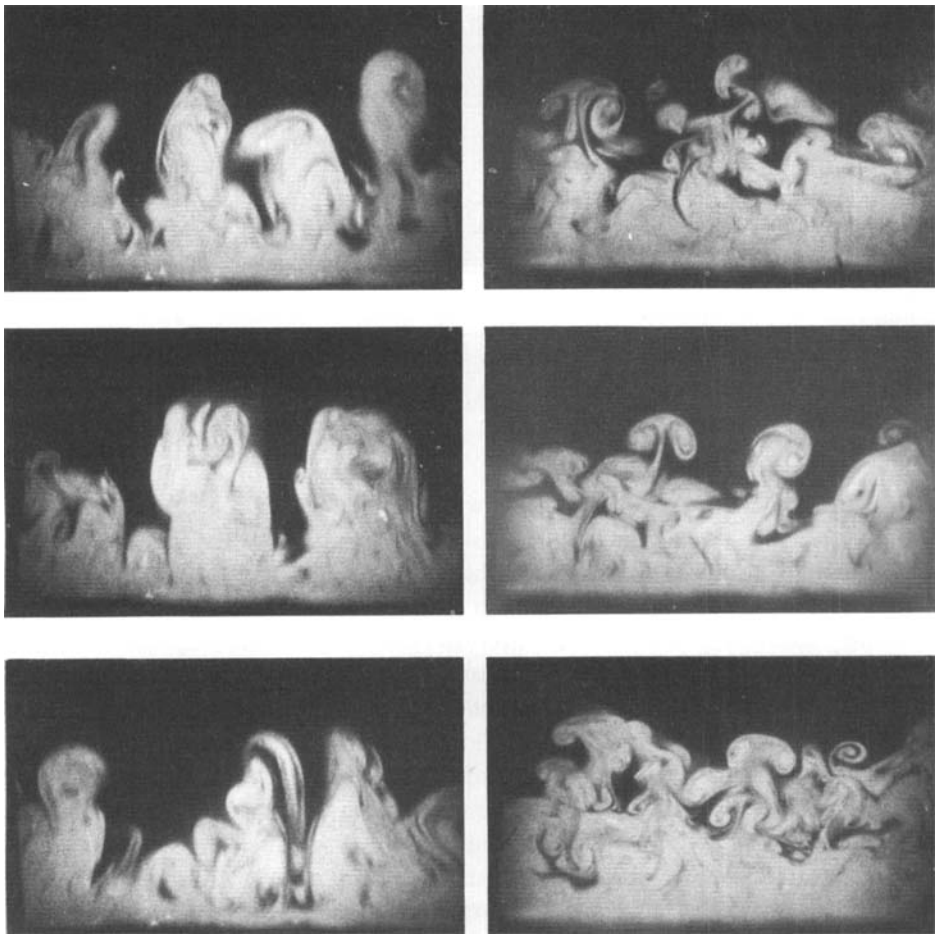

FIGURE 21. Comparison between views with transverse light plane inclined at (*a*) 45° downstream and (*b*) 45° upstream. $Re_\theta = 600$.

are now very narrow) appear to have combined to form much larger structures, although in the very outermost part of the layer they again appear as separate entities. It should be pointed out that the boundary layer on the wind tunnel floor at $Re_\theta = 9400$ was noticeably thicker on the centre-line than on either side, and this is reflected in most frames of the ciné film.

Without doing some sort of statistical analysis it cannot be established with certainty that the lateral scales of the hairpins are directly proportional to the length scale characteristic of the wall region, i.e. ν/U_τ, but, on the face of it, with something like an order-of-magnitude reduction in lateral scales between $Re_\theta = 600$ and $Re_\theta = 9400$, such a suggestion does not seem altogether implausible. We shall return to this point later.

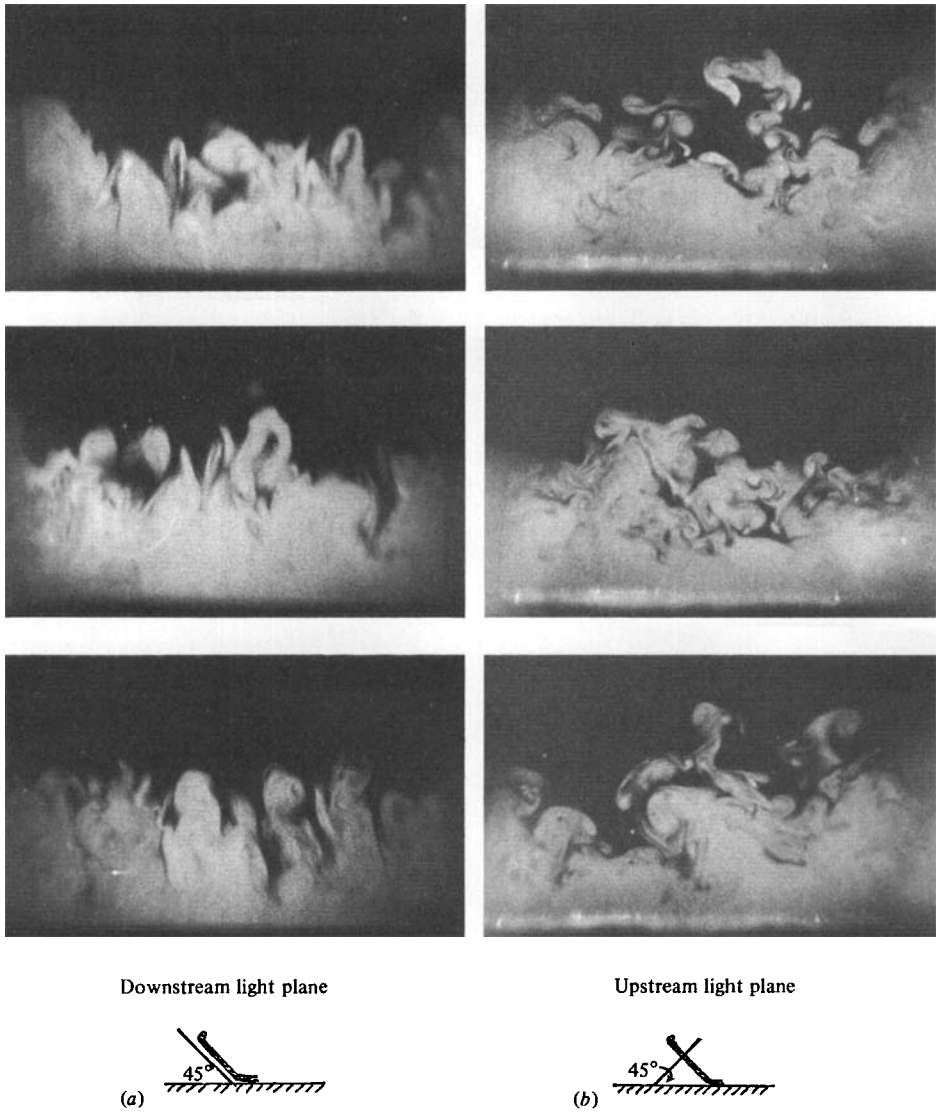

FIGURE 22. Comparison between views with transverse light plane inclined at (*a*) 45° downstream and (*b*) 45° upstream. $Re_\theta = 1700$.

A result which shows up very clearly in the film for $Re_\theta = 1700$, with the light plane inclined downstream, is the appearance of an island as the last trace of a particular feature as it passes the plane of illumination. All features that extend beyond the edge of the boundary layer, as determined from the measured mean velocity profile, disappear in this way, as well as a large number of features that do not extend quite so far. In no case have we observed the appearance of an island preceding the appearance of the remainder of the structure, and we must conclude that the tips of the hairpins are inclined forward into the flow as indicated in the sketch (figure 18). This has important implications, which we shall return to later.

Figure 24 shows a typical sequence of frames where extended features disappear

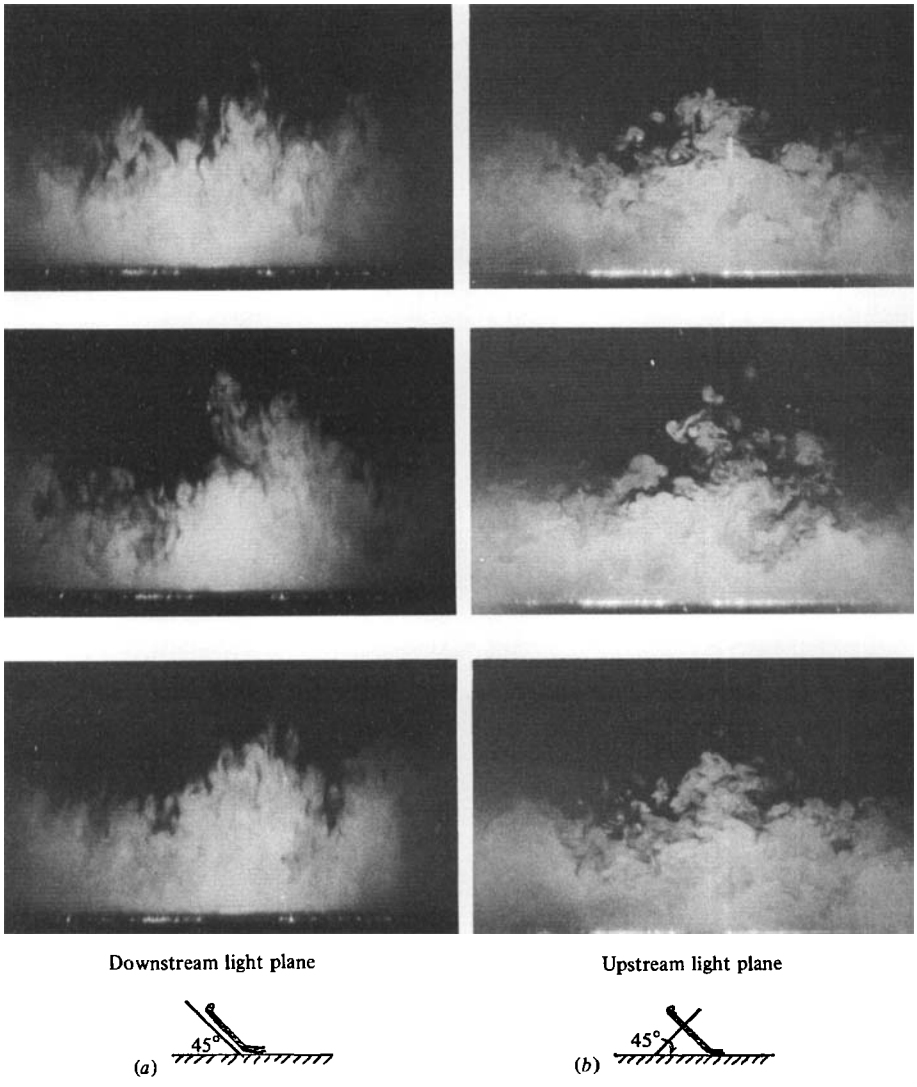

FIGURE 23. Comparison between views with transverse light plane inclined at (*a*) 45° downstream and (*b*) 45° upstream. $Re_\theta = 9400$.

from view leaving smoke-filled islands as their last traces. This is one of the cases where the film itself shows the effect much more graphically.

Several films were made at $Re_\theta = 1700$ with the light plane inclined downstream at angles other than 45°, with the object of determining whether this angle did in fact represent the characteristic angle of the hairpins most closely. Not all the hairpins would, of course, be inclined at precisely the characteristic angle, but it was reasoned that, if the light plane were inclined downstream at appreciably *less* than the characteristic angle, then the features would appear, on the average, to be growing *outwards*, away from the surface while, if it were inclined downstream at a *greater* angle than the characteristic angle, then they should appear to be moving inwards, towards the surface. The sketch (figure 25) is intended to make this clear.

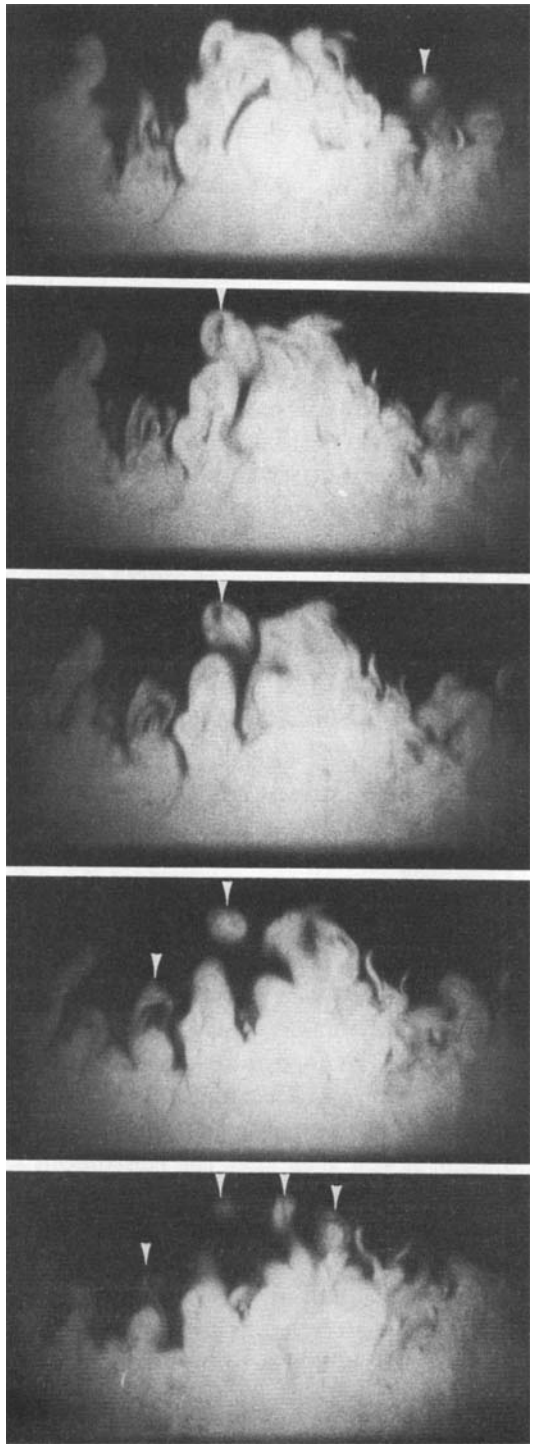

FIGURE 24. Sequence of frames showing disappearing islands.

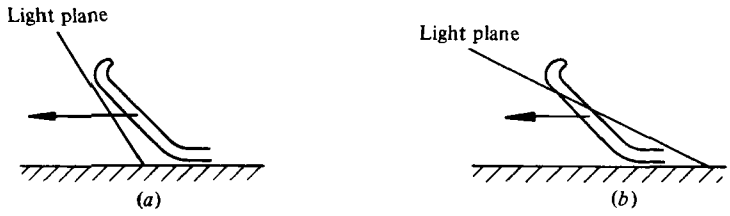

FIGURE 25. Sketch showing effect of varying light-plane inclination. (*a*) Angle of light plane *greater* than characteristic angle: apparent motion *towards* the wall. (*b*) Angle of light plane *less* than characteristic angle: apparent motion *away from* the wall.

With the light plane set at precisely the characteristic angle we should expect to see no apparent overall motion either towards or away from the wall, and if the features had been quite straight then we should not expect to be able to distinguish whether the film were being run forwards or in reverse. In fact, however, the curvature of the tips of the hairpins proved something of a distraction and the results of simply viewing the films were inconclusive. Certainly, with the light plane inclined at 60° there was a very definite apparent movement towards the surface, but no very obvious conclusions could be reached from comparing the films with the light plane inclined at 40°, 45° and 50°. This point might be worth exploring further, but in fact the longitudinal sections seem to have made it clear that the characteristic angle lies in the range 40–50° (see figure 15).

5.3. *Flow in the immediate vicinity of the wall*

The foregoing results would seem to have demonstrated fairly conclusively that vortex loops and hairpins are a dominant feature of the turbulent boundary layer at all Reynolds numbers covered in the experiments, and the results for the lowest Reynolds numbers (say, for $Re_\theta = 600$) show that the loops originate very close to the wall. Unfortunately, details of the flow in the immediate vicinity of the wall cannot be readily distinguished with the flow-visualization technique as used up to this point, so that we cannot directly connect the formation of vortex loops or hairpins with events occurring in, or very close to, the viscous sublayer.

In an effort to clear up this point, smoke was injected tangentially into the sublayer through a rearward-facing slit in the floor of the smoke tunnel about 3 m downstream of the trip at roughly the position where the experiments with the inclined light planes had been performed. Conditions corresponded roughly to an Re_θ of 500.

With general illumination it was seen that the continuous sheet of smoke issuing from the slit soon broke up into a series of streamwise filaments. After travelling more or less parallel to the surface for a substantial distance these filaments left the surface, apparently at random, to become (apparently) generally turbulent. Although the appearances were not encouraging, in that there was no obvious evidence of the formation of vortex pairs, and the filaments could not readily be seen as developed vortices or the spaces between pairs, it was thought worth while to take some 35 mm photographs with a transverse vertical light plane at a position where some of the filaments were breaking away from the wall.

To our surprise, some of these photographs showed well-developed vortex motions and unmistakable examples of vortex pairs (see figure 26). Even where the situation

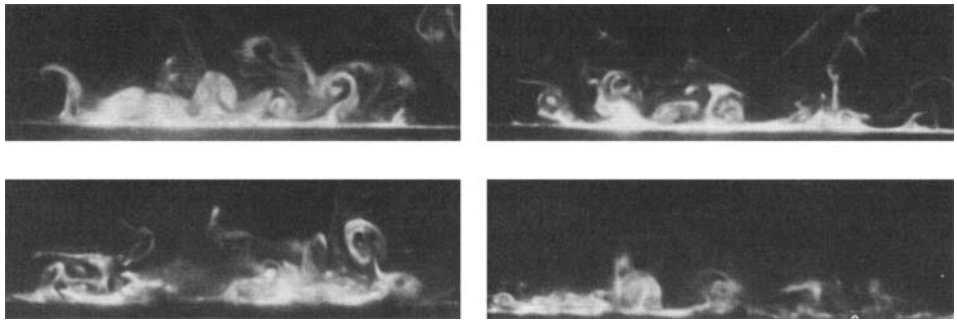

FIGURE 26. Examples of longitudinal vortices and vortex pairs in near-wall region.

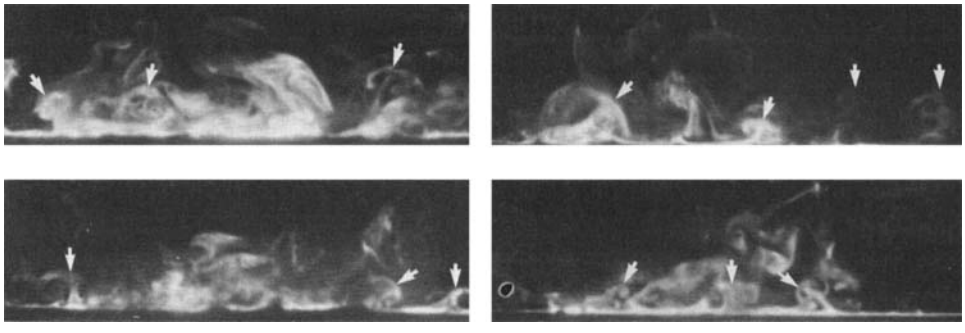

FIGURE 27. Distinguishable vortex pairs in apparently chaotic flow in near-wall region.

was apparently quite chaotic, vortex pairs could still very often be distinguished (see figure 27).

Further work in this area is evidently still required, but the present results certainly provide visual evidence for the ideas of Willmarth (1975, 1978), Blackwelder (1978) and Kreplin & Eckelmann (1979), and make it seem very likely that the hairpins or vortex pairs that we suggest are a prominent feature of the boundary layer as a whole have their origin in longitudinal vortex motions very close to the wall.

5.4. *Mean velocity profiles and skin-friction coefficients*

The present experimental investigation was completed by measuring mean velocity profiles and skin-friction coefficients over the range of conditions in which the ciné films had been made.

In the adapted laboratory tunnel (figure 2) velocity profiles were measured at speeds of approximately 15, 20 and 25 m s^{-1} using a conventional multitube manometer and a Pitot comb. Measurements were made both with the comb resting on the wall and with it slightly raised, so that, as will be seen from figure 28, each profile is defined by two sets of points. Skin-friction coefficients were determined using Preston tubes of two different diameters and the charts of Head & Vasantaram (1971). The coefficients obtained in this way were compared with each other and with those that followed from the H, Re_θ values and Thompson's profile family (Thompson 1967). The appropriate Thompson profiles are also included in figure 28 for comparison.

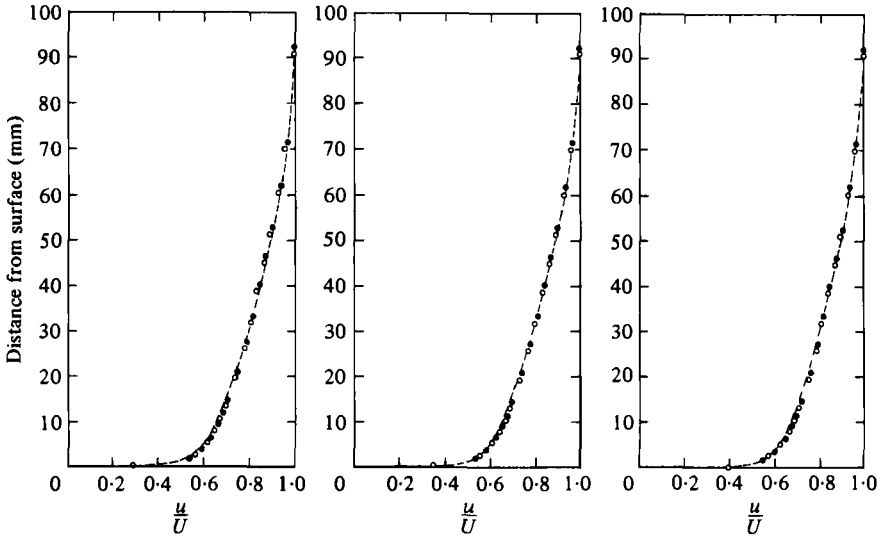

FIGURE 28. Measurements in the laboratory tunnel compared with the Thompson profiles.

	U (m s^{-1})	θ (mm)	Re_θ	H	c_f
(*a*)	15·5	10·4	10620	1·370	0·0024
(*b*)	20·4	10·8	14550	1·370	0·0022
(*c*)	25·5	10·4	17350	1·350	0·0022

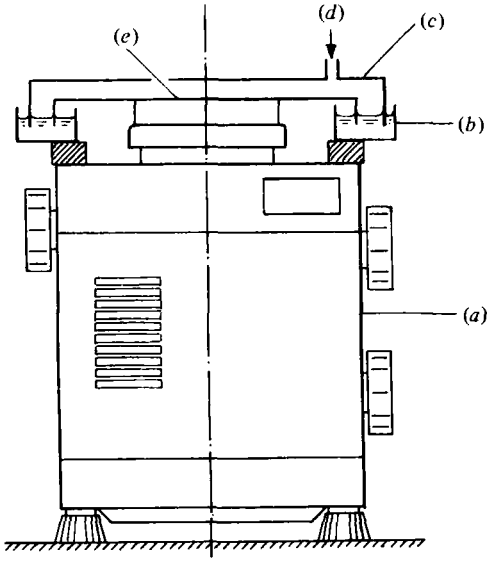

FIGURE 29. Sensitive weighing manometer. (*a*) Sartorius balance (old mechanical type). (*b*) Fixed annular trough containing liquid seal (paraffin). (*c*) Fixed drum supported on annular trough. (*d*) Pressure in. (*e*) Moving drum supported on balance pan.

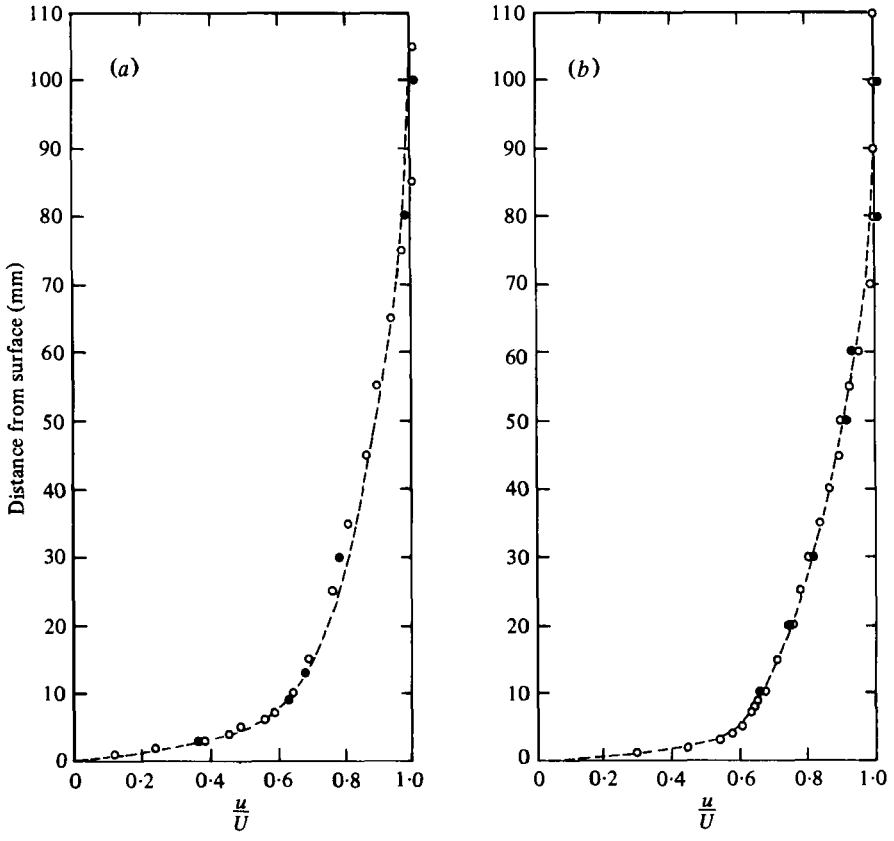

FIGURE 30. Measurements in low-speed smoke tunnel compared with corresponding Thompson profiles.

	U (m s^{-1})	θ (mm)	Re_θ	H	c_f
(*a*)	0·8	10·8	616	1·53	0·0049
(*b*)	2·4	9·5	1570	1·435	0·0037

In the smoke tunnel, speeds were low and velocity profiles were measured at two speeds using a traversing Pitot tube along with the sensitive weighing manometer shown in figure 29.

The velocity profiles measured at approximately 0·8 and 2·4 m s^{-1} are shown in figure 30 along with the corresponding Thompson profiles. Skin-friction coefficients were measured using a single Preston tube and the weighing manometer, and again these measurements of c_f could be compared with the Thompson values.

The results of the measurements are shown plotted in figure 31, where flat-plate curves for H and c_f are also included for comparison (Thwaites 1960).

From figures 28, 30 and 31 it appears that the measurements were quite in accord with those that might be expected for a flat-plate turbulent boundary layer. The small systematic discrepancy between the measured profile and the corresponding Thompson profile at 0·8 m s^{-1} is probably due to inaccuracies of measurement at these very low dynamic pressures.

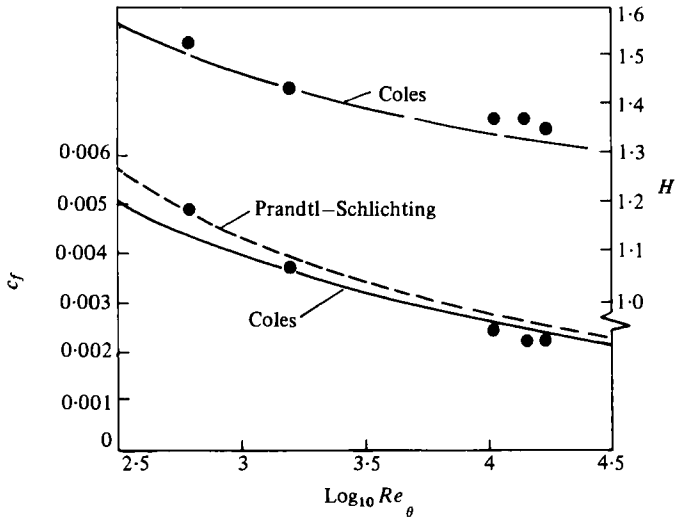

FIGURE 31. Measurements compared with flat-plate curves.

5.5. *Cross-stream dimensions of hairpins*

With values of c_f now available, it was possible to determine the length scale ν/U_τ corresponding to any particular cine film. This length scale would normally be considered relevant only in the wall region of the flow, but on the basis of the present results it might be expected to have a wider significance, possibly bearing some fixed relation to the transverse dimensions of the hairpins or loops throughout the layer.

Of course, at any particular Reynolds number a variety of scales are present, as we have observed, and it is only by a statistical survey that we can deduce with any degree of certainty whether the dimensions of the hairpins do, in fact, scale with ν/U_τ. However, if we indicate the scale of ν/U_τ on individual frames and compare frames from films at different Reynolds numbers we can at least get some idea whether the lateral dimensions of the hairpins vary in the same way with Reynolds number as the length scale ν/U_τ.

In figure 32 we have taken a single frame from each of the three films with a transverse light plane inclined downstream at 45° that we considered earlier (R_θ = 600, 1700 and 9400). On each frame we have indicated the corresponding scale of ν/U_τ, or rather the length representing $100\nu/U_\tau$. (We have been able to do this because the absolute scale of the boundary-layer picture is known from the grid that was photographed in the plane of illumination at the beginning of each film.)

It will be seen from the comparison of the frames at the three Reynolds numbers that the reduction in cross-stream dimensions of the hairpins does in fact seem very closely to parallel that of the ν/U_τ scale. Of course these are only single frames and a variety of hairpin scales are present in each, but we are probably justified in saying that there is nothing in the present results to contradict the idea that the lateral dimensions of the hairpins scale roughly with the value of ν/U_τ. We might even go further and suggest that the lateral dimensions lie for the most part in the range 10–$100\,\nu/U_\tau$.

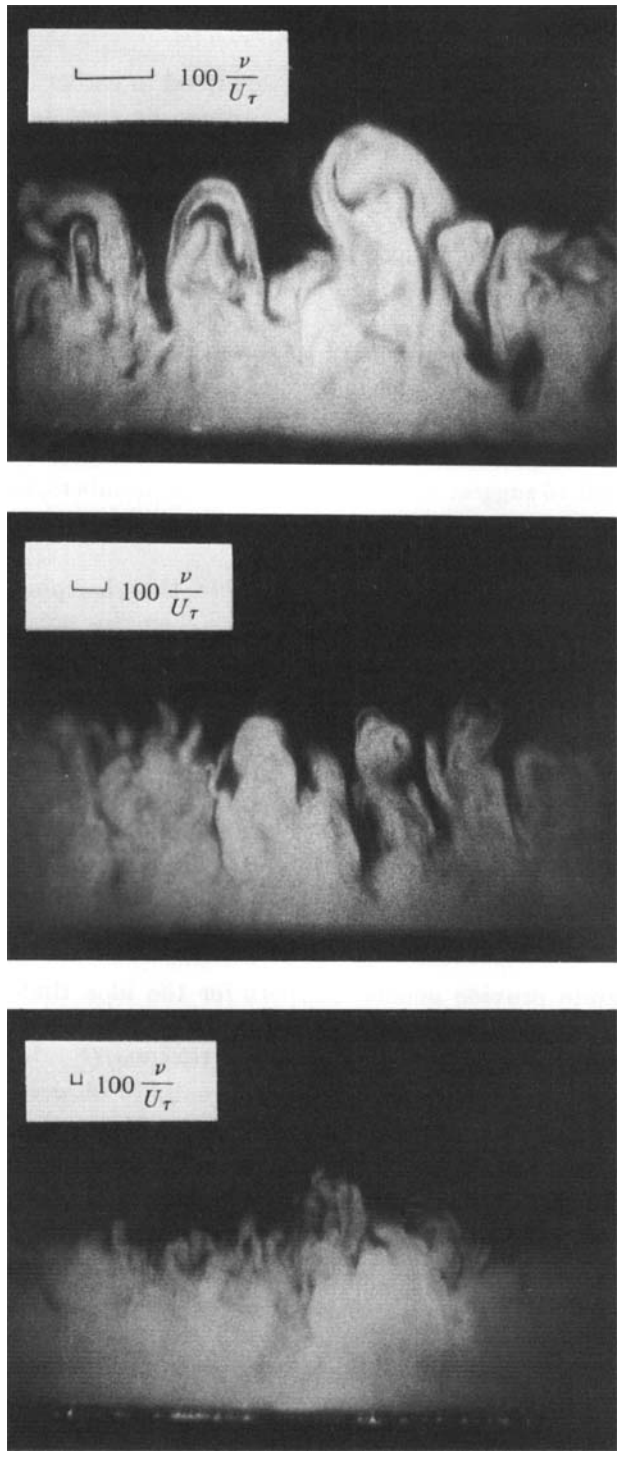

FIGURE 32. Sections of boundary layer with 45° downstream plane of illumination and scales of ν/U_τ indicated.

6. General discussion

6.1. *Summary of results*

We may summarize the experimental results described in earlier sections as follows.

It appears to be established that hairpin vortices, or stretched vortex loops or vortex pairs, are a major constituent of the turbulent boundary layer at all Reynolds numbers. Furthermore it appears that these stretched vortex loops are substantially straight over a large proportion of their length and inclined to the surface at a characteristic angle of something like 45°. This follows from the observations both with a longitudinal light plane and with a transverse light plane inclined downstream at the appropriate angle.

It is also observed from the records with transverse light planes that, for $Re_\theta = 9400$ and presumably at higher Reynolds numbers, vortex pairs or hairpins are noticeably sparser in the outermost regions of the boundary layer and of very small dimensions in cross-section.

Figures like 23 and 15 suggest that, at these Reynolds numbers, large-scale features are made up of very many small-scale hairpins so that the instantaneous edge of layer presents a typically ragged appearance.

There is some evidence from figures such as 14 that hairpins are occasionally produced in a regular sequence, so that the locus of their tips presents a more or less straight line inclined to the surface at a characteristic angle which is smaller than that of the individual hairpins.

A limited investigation of the flow in the immediate wall region shows the existence of longitudinal vortex motions which erupt, apparently at random, to form (in many cases) readily distinguishable vortex pairs. Nevertheless, the connection between the wall region flow and the inclined vortex loops observed further out in the layer cannot be said, at this stage, to be firmly established.

Measurements of mean velocity show that the velocity profiles conform in all important respects to those for a normal turbulent boundary layer in zero pressure gradient.

The present results provide general support for the idea that the cross-stream dimensions of the hairpins scale approximately with ν/U_τ, and further suggest that the typical transverse dimension lies in the range 10–$100\nu/U_\tau$.

The foregoing may be regarded as the direct results of observation, with only a minimum of inference. Before proceeding further it is of interest to see how they fit in with the observations of other experimenters.

6.2. *Comparison with other authors' results*

Even a superficial reading of recent papers on the structure of turbulent boundary layers reveals a surprising number of points of correspondence with the results presented here. These we shall briefly discuss.

Referring to the flow in the immediate wall region, Blackwelder (1978) mentions the experiments of Hama (as reported by Corrsin 1957) which first showed the existence of streamwise streaks, and the flow-visualization experiments of Kline *et al.* (1967) which suggested that the streaks had a spanwise spacing in the region of $100\nu/U_\tau$. Blackwelder (1978) then cites later evidence showing that this spacing is a

random variable with a mean value of approximately $80\nu/U_\tau$. Coles (1978) discusses the origin of the streaks and proposes a mechanism for the production of streamwise vortex pairs in the sublayer based on Taylor–Görtler instability, a suggestion also put forward by Brown & Thomas (1977).

Very much earlier, Bakewell & Lumley (1967) had asserted that 'the dominant structure within the wall region consists of randomly distributed counter-rotating eddy pairs of elongated streamwise extent'.

The relation between the streamwise streaks (or longitudinal vortex pairs) and the 'bursts' and 'sweeps' described by Kline and his colleagues has been the subject of detailed investigation by many experimenters (see, for example, the review paper by Kline 1978), but the picture that has emerged is not altogether clear. Smith (1978) states that these vortex pairs 'are essentially the "legs" of the lifted vortex-loop model of a burst proposed by Offen & Kline (1973)', while Willmarth (1978) describes a flow model 'which consists of hairpin shaped vortices produced by the lifting and stretching of initially *spanwise* vorticity' (present authors' italics). There is no obvious conflict between these two statements, and the flow-visualization film of Brown (undated), showing transition on an axisymmetric body, presents very clear evidence that transition of the laminar boundary layer occurs as a result of the warping of cross-stream concentrations of vorticity (see also Hama, Long & Hegarty 1957).

Further, as regards turbulent spots in the laminar boundary layer, it seems highly probable that the streamwise streaks that follow the passage of a spot (see, for example, figures 4–6 of Cantwell, Coles & Dimotakis 1978) represent the trailing legs of the hairpins occurring in the spot.

So long, then, as we are willing to identify processes occurring in the laminar boundary layer with apparently similar processes occurring in the viscous sublayer of the fully turbulent layer, there would seem to be no reason to doubt the substantial correctness of both Smith's statement quoted above and the model proposed by Willmarth. The only cause for uneasiness would seem to lie in the apparently universal occurrence of streamwise concentrations of vorticity in the viscous sublayer (see, again, the paper by Cantwell *et al.* 1978), with the complete absence of any direct evidence of similar concentrations of spanwise vorticity.

We conclude that the observations in the wall region agree in showing the existence of streamwise streaks that occur at spacings generally similar to the cross-stream dimensions of the vortex loops or hairpins we have photographed further out in the layer (i.e. dimensions on the order of $100\nu/U_\tau$). It also seems reasonable to infer that the occurrence of a burst can be equated to the lifting of a vortex loop from the surface. What is still not clear is whether the loops arise from pre-existing *streamwise* concentrations of vorticity or from the warping of *transverse* vorticity (or, conceivably, from the joint action of both).

Turning now to the outer region of the boundary layer, certain points seem clear. First, it would seem reasonable to equate Falco's 'typical eddies' (Falco 1978) with longitudinal sections of the tips of our hairpins. It then becomes unnecessary to postulate any type of instability other than that arising in the immediate wall region where the hairpins are produced. The scaling of the dimensions of the typical eddies with the wall variables U_τ and ν remarked upon by Falco is also explained. The conclusion by Antonia (1972) that 'there seems to be little doubt that large scale bursts (of high shear stress) observed near the outer region of the boundary layer originate

from or at least extend through to the inner region of the flow' now seems eminently reasonable, particularly since Falco has identified these 'large-scale' bursts with his own typical eddies.

Both Blackwelder and Willmarth in their papers presented at the 1978 AFSOR/Lehigh Workshop quote the work of Chen (1975) who used a rake of ten wires to obtain simultaneous temperature traces at different levels in the boundary layer. Simultaneous velocity traces were also recorded. Despite obvious detailed similarities between the traces in each case, the authors fail to reach the conclusion arrived at here, that the similarities are due to long narrow features extending through at least a substantial part of the boundary-layer thickness. Instead, particularly sharp changes in the traces which extend over the full height of the rake are taken as defining internal fronts which near the wall are associated with the bursting phenomenon. It would appear in fact that the basic results of Chen & Blackwelder (1978) (but not necessarily their interpretations) are in every way compatible with those presented here and provide, in effect, quite independent confirmation.

Brodkey (1978) and his colleagues (see, for example, Praturi & Brodkey 1979), have used stereoscopic flow visualization and simultaneous anemometry to investigate turbulent boundary-layer structure in water. Their experiments were performed at a very low Reynolds number, and their results can readily be interpreted in terms of the low-aspect-ratio vortex loops we should expect to encounter in these circumstances (see figure 17). This would explain the prevalence of transverse vortices that form a notable feature of their sketches.

We shall now look briefly at Theodorsen's paper of 1952 which appears to have been more often referred to than critically examined or explained. The paper is of particular interest here, since it predicts not only the formation of horseshoe vortices, but also the angle at which they should occur, namely 45°, which is just the angle (as near as can be judged) that we have been led to by direct observation. We have not found Theodorsen's arguments easy to follow but it is believed that the following gives a fair account of his ideas.

The basic physical reasoning that appears to underlie his analysis is that vortex stretching provides the only mechanism by which initial concentrations of vorticity in a substantially parallel flow can be further enhanced to provide the origins of turbulence. Since such stretching cannot occur in *strictly* two-dimensional flows then such flows must remain stable, Tollmien–Schlichting analysis notwithstanding.†

If any degree of three-dimensionality is present the situation is otherwise, and the vorticity equation contains an additional term which implicitly represents the result of vortex stretching and so can account for the intensification of vorticity that must precede and accompany the production of turbulence. If the equation is multiplied through by ω (which is now a vector quantity with x, y and z components) we obtain an expression for $D(\frac{1}{2}\omega^2)/Dt$. In tensor notation this may be written (Batchelor 1967) as

$$\frac{D}{Dt}[\tfrac{1}{2}\omega_i\omega_i) = \omega_i\omega_j\frac{\partial u_i}{\partial x_j} + \omega_i\nu\nabla^2\omega_i,$$

† In this analysis, the basic shear flow remains parallel and invariant with distance and concentrations of vorticity can arise only through the periodic disturbances that are superimposed. Theodorsen argues that, in the absence of three-dimensionality, these concentrations can only *decay* due to the diffusive action of viscosity, just as they would in a fluid at rest, and goes to some lengths to justify this view.

where the first term on the right is the one in which we are interested and which does appear in strictly two-dimensional flow.

Following Theodorsen, we now consider a shear flow (in a long, wide parallel channel, for example) where the basic flow is substantially independent of downstream distance and distances transverse to the flow and parallel to the wall. We can replace x by s, the distance along a streamline, and y by n, the distance normal to the wall, with z the distance transverse to the flow. In this basic flow we consider that we have embedded a concentration of vorticity with components ω_s, ω_n and ω_z. These may be of similar magnitudes, but from the nature of the basic flow $\partial u/\partial n$ is very much greater than any other of the velocity derivatives. Thus, to a close approximation, the stretching term (or turbulence term, as Theodorsen calls it) will be simply

$$\omega_s \omega_n \frac{\partial u}{\partial n}.$$

This will be a maximum when the component of the vorticity vector in the s, n plane is inclined at 45° to the main flow direction.

The foregoing reasoning would seem quite sound, but the deduction that the breakdown of laminar flow and the production of turbulence generally should be accompanied by the formation of horseshoe vortices inclined downstream at this 45° angle would seem to require further justification. In part this is provided by Theodorsen, who shows that horsehoe vortices with a downstream inclination satisfy many of the physical requirements that might be imposed, but, so far as the present authors are concerned, the question still remains open as to why the horseshoes should set themselves at the angle which makes their contribution to turbulence production a maximum. We shall return to this question later. Here we may simply suggest that Theodorsen's paper shows a remarkable degree of physical insight, with implications that have been very largely neglected. The only major point at which his results appear to be contradicted by the present observations lies in his statement that the primary turbulent structure (the horseshoe vortex) is similar in pattern and differs only in scale: our results would seem to demonstrate quite conclusively that two different length scales (ν/U_τ and δ) are involved, so that the form of the horseshoes is very much dependent upon Reynolds number.

Turning now to the paper by Black (1968) we find an approach which is quite different from that adopted by Theodorsen (1952) although the final picture is not dissimilar. The starting point of Black's analysis is the assumption that the viscous sublayer is subject to periodic breakdown as Einstein & Li (1956) had suggested earlier, and this periodic breakdown is the result of an instability which moves upstream relative to the local flow velocity and which grows and decays, as it moves downstream in an absolute sense, each instability pattern during its lifetime giving rise to a sequence of horseshoe vortices. The lateral dimensions of these vortices and the frequency with which they are shed are clearly envisaged by Black as scaling with the wall variables U_τ and ν, and he specifically states that the largest vortex systems present will define the edge of the boundary layer. He is thus led to the conclusion that the quantity $\delta U_\tau/\nu$, which varies strongly with Reynolds number, is a key parameter in defining the turbulence structure of the layer. All these ideas are in excellent accord with the present observations; in particular the occurrence of inclined interfaces that are apparently the envelopes of the tips of individual hairpins

(see figure 14) lends support to the idea that, at least occasionally, hairpin vortices are formed in a regular sequence, and the physical mechanism of Black's instability may be that described briefly towards the end of §5.1. Black's analysis is not easy to follow and we have not attempted to outline it here. Whether or not his intuitive arguments are always sound, there can be no doubt that his conclusions, like those of Theodorsen, show a remarkable degree of insight.

Incidentally it may be remarked here, apropos of figure 14, that the interfaces indicated on the figure make an angle to the surface that is not too different (20° as compared to 18°) from that which Brown & Thomas (1976) gave as the angle along which correlations are a maximum. Although such features occur (it would appear from our results) only relatively rarely, this is not significant if signals are sampled only when the correlation exceeds a stipulated high value, as was the case in at least some of the experiments of Brown & Thomas. Certainly, along such an interface we should expect correlations to be very high indeed.

Overall, it would appear that the observations of other experimenters fit very well into the framework we have provided. Many questions remain to be answered but it seems likely that they should be well posed and appropriate questions.

Before leaving the work of other authors, we should like to quote from a review paper by Saffman (1977). Towards the end of his introductory section he writes

> Finally we should not altogether neglect the possibility that there is no such thing as 'turbulence'. That is to say it is not meaningful to talk of the properties of a turbulent flow independently of the physical situation in which it arises. In searching for a theory of turbulence, perhaps we are looking for a chimera. Turbulent phenomena of many types exist, and each one of practical importance can be analysed or described to any degree of detail by the expenditure of sufficient effort. So perhaps there is no 'real turbulence problem', but a large number of turbulent flows and our problem is the self-imposed and possibly impossible task of fitting many phenomena into the Procrustean bed of a universal turbulence theory. Individual flows should then be treated on their merits and it should not necessarily be assumed that ideas valid for one flow situation will transfer to others. The turbulence problem may then be no more than one of cataloguing. The evidence is against such an extreme point of view as many universal features seem to exist, but nevertheless cataloguing and classifying may be a more useful approach than we care to admit.

In the light of the present results this does not seem such an extreme point of view, and we have certainly seen that, in the case of the turbulent boundary layer in zero pressure gradient, the simple change of viewpoint obtained by using transverse light planes inclined at 45° has greatly reduced the apparent level of randomness, and what we now see is a relatively ordered structure of extended vortex loops. A considerable degree of disorder is still of course present, but the concept of turbulence as the random motions of small parcels of fluid would now seem quite untenable in the boundary-layer context.

7. Further considerations

7.1. *Lifetime of hairpins*

(i) *Dissipation.* In two dimensions, a vortex pair in a viscous fluid will be subject only to dissipation, as the vorticity from each vortex diffuses outward and cancels that from the other vortex. The effective lifetime of the pair (we might expect) will be very much less than the lifetime of either vortex in isolation, since the pair will effectively die once the two cores of near-solid-body rotation have grown sufficiently to interpenetrate. We might therefore expect that the velocity that each vortex induces in the other will progressively decay as the diffusion of vorticity proceeds, and will decrease rather abruptly when the final stage of interpenetration has been reached.

Insofar as the vortex pair may be taken to represent the cross-section of an extended vortex loop, its characteristics will be related to the variables U_τ and ν, and we might expect the lifetime of an average vortex pair to be measured by ν/U_τ^2. The induced velocities associated with the vortex pair will similarly be related to U_τ, and the time for the vortex loop to extend itself across the layer will be measured by δ/U_τ.

The ratio (time to grow across boundary layer)/(lifetime) we should then expect to be measured by

$$\frac{\delta}{U_\tau}\frac{U_\tau^2}{\nu} = \frac{\delta U_\tau}{\nu} = \frac{U\delta}{\nu}\left(\frac{c_f}{2}\right)^{\frac{1}{2}},$$

the parameter that Black (1968) had postulated as being of particular significance.

At high Reynolds numbers, this quantity will become very large, and ultimately we should expect (on the basis of the arguments presented so far) that a stage will be reached where extended vortex loops will no longer survive to penetrate the outermost regions of the layer. This, however, neglects certain points which may be relevant and which we shall now briefly discuss.

(ii) *Variation in scales.* If vortex loops are produced in the immediate wall region, then it is only on the average that their scales will be related to the (mean) friction velocity U_τ. Some loops will have much longer potential lifetimes than others, and, in principle, it seems at least possible that, however high the Reynolds number, there will always remain a diminishing minority of loops that are capable of extending throughout the layer.

If vortex pairing can occur in the wall region, due to vortex loops of low aspect ratio wrapping around each other, then the range of scales to be expected will considerably increase.

In the light of these observations it is interesting to note that the cross-stream films for $Re_\theta = 9400$ (see figures 23 and 32) show vortex loops that are very noticeably sparser in the outer region than close to the wall, and also (possibly) of somewhat larger cross-stream dimensions than a simple scaling with ν/U_τ would suggest.

(iii) *Stretching of vortex pairs.* If an already elongated vortex loop (hairpin) is further stretched, then we should expect the concentrations of vorticity in the cores of the vortices to be increased and considerations of continuity suggest that the distance between the cores should decrease. Since the circulation around each limb

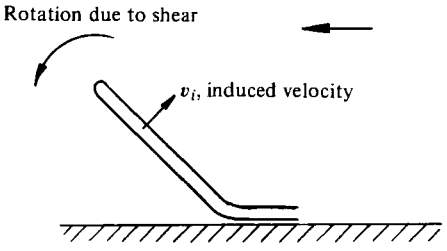

FIGURE 33. Hairpin growing out from wall at characteristic angle. The feature can only remain at fixed angle to the wall if v_i increases outward to counter rotation due to shear.

of the hairpin remains unaltered in the stretching process, the decrease in the distance between the cores (if it occurs) must be accompanied by a corresponding increase in induced velocity. Thus we see that stretching provides a possible mechanism by which induced velocities can be maintained, and even increased, in the presence of dissipation.

It seems inevitable, in fact, that hairpin vortices growing out from the wall and inclined downstream at an angle of something like 45° should be subjected to stretching (indeed it would seem at first sight that 'growth' and 'stretching' should be virtually synonymous in this context). In a shear flow parallel to the wall, the downstream angle of 45° represents the direction of the principal axis, along which the strain is one of pure extension and the rate of stretching is a maximum, and it must surely be significant that the characteristic angle of the hairpins is so close to this value. The following is a possible explanation.

Let us consider a hairpin at some particular stage of its growth as shown in the sketch (figure 33).

The direct effect of the shear flow will be to rotate the hairpin back towards the wall, and this effect can only be resisted by the induced velocity that each limb of the hairpin imposes on the other. The angle at which the hairpin sets itself will thus be the result of these two conflicting effects. Initially the angle may be greater than 45°, but at some stage dissipation will reduce the induced velocities and the hairpin will be rotated back towards the 45° angle. At the same time the rate of stretching will increase, and so tend to increase the induced velocity; thus, so long as the angle that the hairpin makes with the surface is *greater* than 45°, the situation remains stable. Once the hairpin has been rotated to an angle *less* than 45°, however, the rate of stretching will decrease and there will be nothing to prevent the angle decreasing further, with ever-increasing rapidity, as dissipation proceeds.

On this argument, then, we might expect to see large numbers of active hairpins at angles of 45° or greater but relatively few at smaller angles. This does not conflict too drastically with observation, but on the other hand there is no direct evidence that stretching of the hairpins does in fact bring the limbs closer together with a corresponding increase in the induced velocity.

These rather inconclusive speculations suggest the need both for further experiments at high Reynolds numbers and for greater insight into the behaviour of stretched vortex pairs in a viscous fluid.

7.2. *Flow in the wall region*

The evidence for the universal law of the wall, at least for incompressible flow in zero pressure gradient, seems virtually unassailable, and we should expect the universality of the mean velocity distribution to be matched by a corresponding universality in the turbulence structure. This implies that we should have a universal (or effectively universal) distribution of loops, horseshoes and hairpins (in ascending order of aspect ratio, as indicated in figure 17) in the wall region, *independent* of Reynolds number, and this in turn implies that only a minority of the loops generated at the wall should survive into the outer region of the layer. We may speculate that in the law-of-the-wall region the mean length of the hairpins will be proportional to ν/U_τ (i.e. that they will have a mean aspect ratio), while in the outer region the mean length of the hairpins will be determined by the thickness of the layer.

This of course does not explain in any obvious way why the universal law of the wall should take the form that it does, although there is the hint that, close to the wall, the circulatory flow fields due to the loops (or horseshoes or hairpins) may be restricted by the presence of the wall and directly proportional to distances from it, in accordance with the mixing-length relation $l = ky$. Well away from the wall, however, the momentum transport in the layer may be due less to the circulatory flow fields of the hairpins than to the growth of the hairpins directly transporting low-momentum fluid across the layer and leading to a mixing length that is proportional to δ. These, however, are the merest speculations and we shall not pursue them further here.

7.3. *Entrainment*

Figure 34 (*a*, *b*) shows how mainstream fluid is entrained into the boundary layer at low Reynolds numbers, and is in accordance with the description given by Bevilaqua (1977) and the sketch (figure 35).

At these very low Reynolds numbers it is scarcely possible to distinguish between large- and small-scale motions, and the large eddies appear to be composed of either single vortex loops or of combinations of relatively few such loops. From the ciné film, of which figure 34 shows single frames, the large eddies appear to be in a relatively brisk state of rotation.

Although direct visual evidence is lacking at high Reynolds numbers, we may expect that the tips of the hairpins will behave in much the same way as the vortex loops close to the wall observed at low Reynolds numbers, so that entrainment is taking place by the same mechanism but at a very much reduced scale relative to the boundary-layer thickness. A relatively large amount of the rotation will take place in the tips of the hairpins, so that the large-scale structures which appear (in most cases) simply as random agglomerations of such hairpins, will exhibit only the relatively slow overturning motion we have remarked upon earlier.

Figure 36 is intended to illustrate the difference between entraining motions at low and high Reynolds numbers.

It is perhaps worth pointing out here that the apparent slow overturning motion of large-scale features at high Reynolds numbers, which is normally accompanied by equally slow changes in shape, would seem to be quite compatible with such features being largely composed of 45° hairpins, so long as the lifetimes of these hairpins are relatively short.

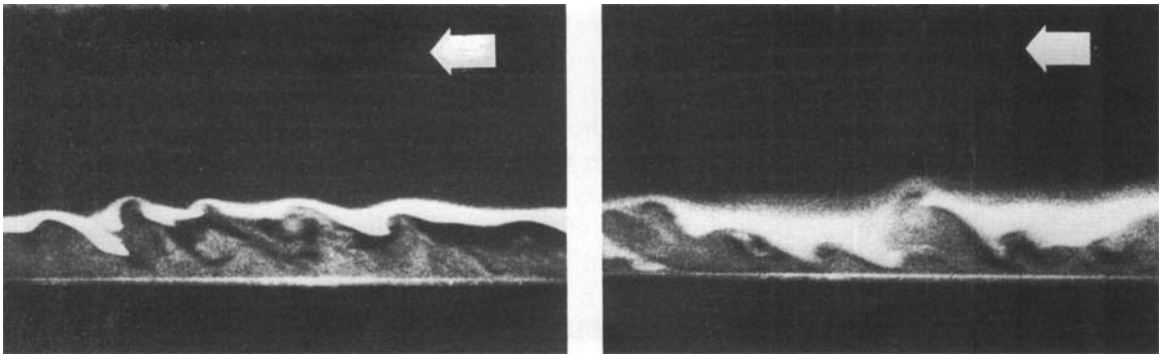

(*a*) (*b*)

FIGURE 34. Entrainment at a low Reynolds number ($Re_\theta \simeq 500$). (*a*) Narrow smoke filament in stream impinging on boundary layer just upstream of the field of view. (*b*) Thicker smoke filament impinging on boundary layer well upstream; entrainment has proceeded much further.

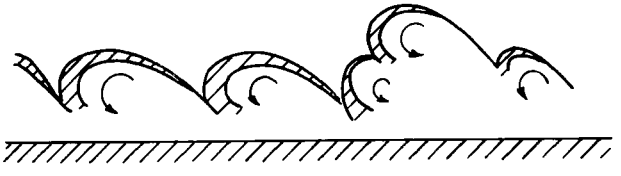

FIGURE 35. Sketch showing entrainment at low Reynolds number. The hatching represents fluid in the process of entrainment.

When considering the ultimate nature of entrainment, which is simply the transfer of vorticity to hitherto irrotational fluid, it should be borne in mind that the transfer of vorticity on a molecular scale takes place with very much greater facility than the transfer of even very small oil droplets, so that some caution should be exercised in identifying the edge of a smoke-filled region with the instantaneous boundary-layer edge or the precise limit of the rotational flow. Beyond the edge of the smoke, there will evidently be a small but finite region which is not entirely free of mean or fluctuating vorticity. Conversely the presence of smoke will not necessarily imply the presence of mean or fluctuating vorticity, since vorticities of opposite sign may fortuitously cancel in a particular region, but there is no similar mechanism by which the concentration of smoke in this region can be reduced. At the same time, any region where the cancellation of vorticity takes place will normally be within the boundary layer, and there will be some net residue of vorticity in the cross-stream direction which will not make the presence of smoke wholly misleading.

Generally speaking, it would seem that the smoke gives a very fair indication of the distribution of concentrations of vorticity, but we should avoid positively identifying (say) narrow smoke-free fissures or pockets as regions wholly free from vorticity.

The question of entrainment and the spread of vorticity is discussed in general terms in the paper by Head & Bradshaw (1971).

FIGURE 36. Sketch comparing entraining motions at (*a*) low and (*b*) high Reynolds numbers. (*a*) Entrainment proceeding on scales comparable with boundary-layer thickness. (*b*) Entrainment proceeding on scale of hairpin tips.

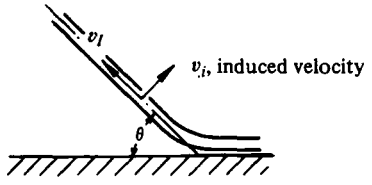

FIGURE 37. Sketch showing the motion of a hairpin close to the wall. If features remain substantially straight, and at a fixed angle of approximately 45° to the wall, then v_i, the velocity along the vortex axis, $\simeq v_i$.

7.4. *The growth of hairpins*

We have said earlier that the growth or elongation of hairpins may at first sight be identified with the stretching they must undergo when aligned (approximately) with the direction of maximum strain, but this may not provide the complete explanation. If we look at the sketch (figure 37) we see that part of the growth may arise from the induced velocities 'peeling' vortex pairs up and away from the surface, so that the hairpins may be (so to speak) fed from below. For this to occur, the hairpins must be moving upstream relative to the vortex pairs from which they originate. So far as the present authors are concerned it remains an open question whether the growth of hairpins is due primarily to stretching or to the process we have just described.

Another question that remains unanswered is why the hairpins grow out from the surface due to the induced velocities just so far and no further, but here we can provide a tentative explanation. The problem is really to explain why, on the simple argument of induced velocities and the observations from longitudinal sections that the hairpins remain substantially straight (see figure 37), the hairpins do not continue to grow indefinitely, well beyond the boundary edge at any particular Reynolds number. The answer we propose is that growth can continue only so long as the hairpins remain in a region of shear. This suggestion is based on the following observations.

(i) When we see hairpins that have developed into a region that is free from shear we find that the tip curls over into the stream and inhibits further growth. This appears to happen occasionally in the formation of turbulent spots, and an example

FIGURE 38. Example of curled-over hairpin in developing spot.

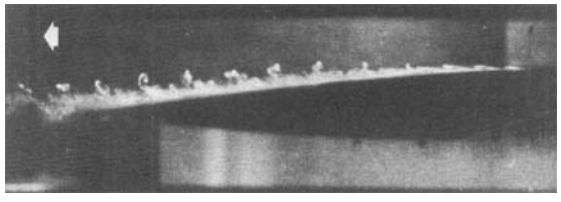

FIGURE 39. Succession of curled-over hairpins photographed by Bergh (1957).

is shown in figure 38. A somewhat different case is shown in figure 39 which is a reproduction of a figure given by Bergh (1957). Here it appears that a regular train of hairpins has been produced by periodic disturbances, and these all exhibit the same property of rolling up into the stream and being arrayed at a mean angle to the surface that is markedly greater than the angle that is characteristic of the hairpins in the fully developed turbulent layer.

(ii) The second observation is one that has been remarked upon earlier, namely that, with a transverse light plane inclined downstream, the last trace of a hairpin appears as a smoke-filled island in the flow. This would seem to provide convincing evidence that the development of hairpins in the turbulent boundary layer at moderate Reynolds numbers ($Re_\theta \simeq 2000$ say) terminates with the turning over of the tip into the flow, and this is characteristic, as we have just remarked, of the hairpin penetrating a region of zero shear.

We are thus led to the tentative conclusion that the maximum extent to which the hairpins can grow is limited by the pre-existing strain field; some small measure of further growth must be possible, otherwise the boundary layer would not grow and the strain field extend itself as we move downstream.

We should also note that, at very low Reynolds number, or in the wall region generally, a further limitation on the outward growth of vortex loops or hairpins may be provided by their mutual interaction and entanglement.

8. Conclusions

Leaving on the side the more speculative aspects of the preceding discussion, we may list the conclusions of the present investigation as follows.

(i) The turbulent boundary layer at Reynolds numbers up to $Re_\theta \simeq 10000$ consists

very largely of vortex loops, horseshoes or hairpins arrayed at a characteristic angle of approximately 45° to the wall.

(ii) The cross-stream dimensions of these loops, horseshoes or hairpins scale (at least approximately) with the wall variables U_τ and ν, while their length appears to be limited only by the thickness of the layer.

(iii) As a consequence of (ii) there is a very large scale effect on the structure of the layer.

(*a*) At *very* low Reynolds numbers ($Re_\theta < 500$, say) no very clear distinction can be made between large- and small-scale motions, and the large eddies appear to consist of individual vortex loops or relatively small numbers of such loops interacting. The eddies appear quite rounded and exhibit a relatively brisk rate of rotation for reasons explained in the text.

(*b*) As the Reynolds number increases, at least a proportion of the loops become increasingly elongated, so that they may be better described as horseshoes or hairpins. At $Re_\theta > 2000$ (say) large-scale structures appear to be made up of random agglomerations of such hairpins, and it is, perhaps, misleading to refer to them as large eddies since they do not appear to exhibit any particular coherent motion beyond a relatively slow overturning or toppling due to shear.

(*c*) At high Reynolds numbers ($Re_\theta \simeq 10000$) a small proportion of the loops have become almost incredibly elongated, and in the outermost part of the layer are widely separated in relation to their cross-stream dimensions.

(iv) At the higher Reynolds numbers there is occasional evidence of hairpins being formed in a regular sequence so that their tips lie on a line which makes a smaller angle to the surface than the 45° angle characteristic of the individual hairpins.

(v) There is decisive evidence that the tips of the hairpins are inclined forward into the flow, and this leads to the speculation (for reasons described in the text) that the outward growth of the hairpins continues only so long as they lie in a region of pre-existing shear.

(vi) It is a general conclusion of the investigation that the use of smoke, with light-plane illumination by laser, provides a very satisfactory means of exploring turbulent boundary-layer structure. The full potentialities of the technique remain to be exploited, and it is suggested that the present work should be extended to higher Reynolds numbers and to flows with pressure gradient.

Both authors are indebted to the Science Research Council for financial assistance in the later stages of the work (GR/A/4827·3) and the second author to the Indian Government for earlier support. They are also grateful for the interest shown by Dr A. A. Townsend in the work and to Dr D. J. Maull for helpful discussions.

9. Additional observations

While the present paper was under review, several points arose which we will briefly discuss here.

First, the authors' attention was drawn to a film made by Prof. John Weske in collaboration with Theodorsen in the early 1950's, following the publication of Theodorsen's paper (1952). The experiments were performed in fully developed laminar pipe flow at Reynolds numbers somewhat below the lower critical value of

approximately 2000. A small protrusion on the wall of the pipe triggered the production of regular sequence of vortex loops or horseshoes of the type postulated by Theodorsen. Flow visualization was performed in the main using the tellurium technique, with either a tellurium wire extending across the pipe or the protrusion itself forming the electrode. In some cases dye was also used. Figures 40(*a–d*) show frames from different sequences of the film. Figure 40(*b*) is an oblique view which shows clearly the general form of a single horseshoe, while figures 40(*c, d*) show the interaction of a series of horseshoes with the surrounding fluid. These latter figures have a number of detailed features in common with the low-Reynolds-number boundary layer pictured in figures 16 and 34 (particularly the latter), and provide general support for the suggestion that the boundary layer here consists of relatively small numbers of vortex loops or horseshoes of varying scales.

The authors are grateful to Prof. Weske for making his film available and for reference to an earlier paper (Weske & Plantholt 1953).

It was remarked in §7.1 (ii) that a wide variation in the scales of horseshoes or hairpins might be expected in the wall region, and that it is only in the mean that the scaling with U_τ and ν will apply. A recently published paper by van Maanen (1979) provides convincing evidence that this is the case. By the use of laser-Doppler anemometry in fully developed turbulent pipe flow, the author demonstrates that the time intervals between bursts at a fixed (small) distance from the wall show a wide variation, with the frequent occurrence of bursts with a small time spacing and relatively rare occurrence of bursts with a large time spacing; in fact the distribution is very nearly log-normal, with the log of the frequency of bursts decreasing linearly with increasing time interval between bursts. Van Maanen's results also show that the u' signature of a burst is essentially that of a discrete vortex.

More direct evidence in favour of the hairpin-vortex hypothesis comes from the experiments of Prof. Deckker, where the focused schlieren technique was used in a rectangular duct, to make visible the growth of the boundary layer following the passage of a shock. The paper by Deckker & Weekes (1976) shows spark photographs of the flow on the floor of the duct for two different strengths of shock wave, with different time intervals following the passage of the shock. Where the boundary layer is turbulent, as in the photographs reproduced here as figures 41(*a, b*), quite marked and regular striations are visible in the flow close to the wall. Similar results were obtained at all five shock strengths for which tests were performed.

The angle these striations make with the wall will be seen to vary substantially across the full width of the field of view, but it appears that this variation can reasonably be ascribed to the effects of astigmatism and spherical aberration that arise in offset mirror systems (Holder & North 1963). In the middle of the field of view these effects should be minimal, and figures 42(*a, b*) show enlarged photographs of this region (Deckker 1980).

Figure 42(*a*), like figures 41(*a, b*), shows the boundary layer on the floor of the duct, while figure 42(*b*) shows the boundary layer on a flat plate a relatively short distance downstream of the leading edge. The two photographs were taken simultaneously and at the same position, and differences between them, if not due to optical effects, must presumably be ascribed to leading-edge proximity in the flat-plate case. There is some suggestion that the angles the striations make with the wall in this case are rather closer to the 45° angle of the turbulent boundary layer

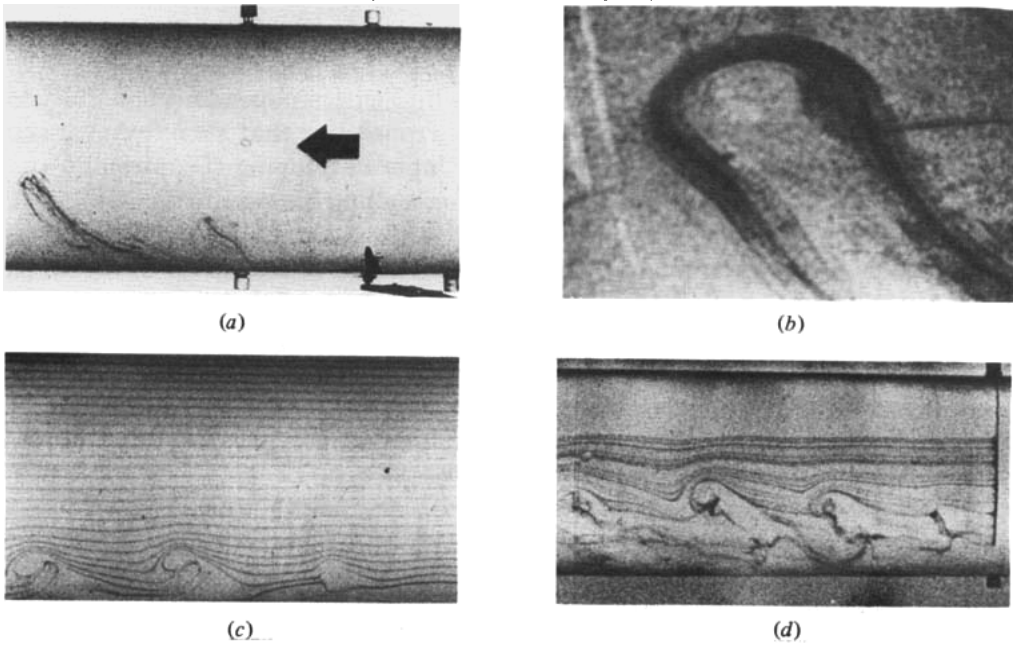

(*a*) (*b*)

(*c*) (*d*)

FIGURE 40. Frames from the film by Weske. (*a*) Horseshoe vortices arising from protrusion on the right. (*b*) Oblique view of single horseshoe. (*c*) Sequence of horseshoes shown by tellurium wire. (*d*) Sequence of horseshoes at somewhat higher *Re*.

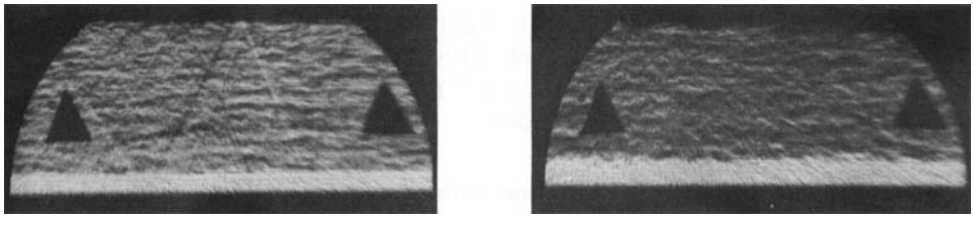

(*a*) (*b*)

FIGURE 41. Flow on floor of duct (Deckker & Weekes 1976). (*a*) 1·40 ms after the passage of the shock (p_{21} = 2·24). (*b*) 2·00 ms after the passage of the shock (p_{21} = 2·24).

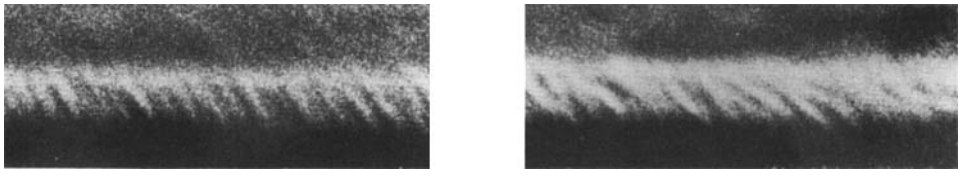

(*a*) (*b*)

FIGURE 42. Enlarged photographs of flow (*a*) on the floor of the duct and (*b*) on a flat plate (Deckker 1980).

growing in the normal way, rather than the angle of something like 60° made by the striations in the boundary layer on the floor. But, however this may be, the existence of regular, narrow inclined structures in the time-dependent boundary layer would seem, at the very least, to increase the probability that such features should form a constituent of the turbulent boundary layer developing the normal way.

The authors are grateful to Prof. Deckker for making his results available and for helpful correspondence and discussions.

Attention is also drawn to an earlier paper (Frenkiel & Klebanoff 1973) in which the authors suggest, on the basis of a statistical analysis of their hot-wire data, and their observation as to the lack of intermittency in their signals of u' in contrast to the intermittency observed in the signals of $u'v'$ (Kim, Kline & Reynolds 1971), in the region close to the wall, that 'one may speculate that the basic structural elements of a turbulent boundary layer are similar to the hairpin eddies occurring in the transition process as described by Klebanoff *et al.*' Thus, it would seem that the present results are at least compatible with the careful and detailed hot-wire observations of these authors.

Again, the authors are grateful to Dr Dinkelacker for making available a copy of a recent paper (Dinkelacker 1979) in which measured wall-pressure fluctuations are interpreted as being due to pairs of 'tornado-like' vortices being swept along the wall, the vortex pairs arising (it is speculated) from the progressive warping of initially straight concentrations of transverse vorticity.

These quite independent observations, all pointing in the same direction, provide encouraging evidence in favour of the hairpin-vortex hypothesis.

Finally, it should be pointed out that, since this paper was originally submitted, a summarized version has been presented (Head & Bandyopadyay 1979). This contains little that has not been covered in the main text of this paper, but one observation is perhaps worth restating here. It is that 'while vorticities of opposite sign from the two legs of the hairpins may diffuse into each other and cancel, there is no similar mechanism by which the transverse vorticity in the hairpin tips can be destroyed. Thus, at really high Reynolds numbers, it may be only the tips of the hairpins that survive and remain active in the outermost regions of the layer.' This emphasizes the need for further experiments at substantially higher Reynolds numbers.

REFERENCES

ANTONIA, R. A. 1972 Conditionally sampled measurements near the outer edge of a turbulent boundary layer. *J. Fluid Mech.* **56**, 1.

BAKEWELL, H. P. & LUMLEY, J. L. 1967 Viscous sublayer and adjacent wall region in turbulent pipe flow. *Phys. Fluids* **10**, 1880.

BANDYOPADHYAY, P. 1977 Combined flow visualisation and hot-wire anemometry in turbulent boundary layers. In *Structures and Mechanisms of Turbulence I* (ed. H. Fiedler), Lecture Notes in Physics vol. 75, p. 205. Springer.

BATCHELOR, G. K. 1967 *An Introduction to Fluid Dynamics*. Cambridge University Press.

BERGH, H. 1957 A method for visualizing periodic boundary layer phenomena. *IUTAM Symp. on Boundary Layer Research*. Springer.

BEVILAQUA, P. M. & LYKOUDIS, P. S. 1977 Some observations on the mechanism of entrainment. *A.I.A.A. J.* **15**, 1194.

BLACK, T. J. 1966 Some practical applications of a new theory of wall turbulence. *Proc. 1966 Heat Transfer and Fluid Mech. Inst.* Stanford University Press.

BLACK, T. J. 1968 An analytical study of the measured wall pressure field under supersonic turbulent boundary layers. *N.A.S.A.* CR-888.

BLACKWELDER, R. F. 1978 The bursting process in turbulent boundary layer. *Workshop on Coherent Structure of Turbulent Boundary Layers*, p. 211. Lehigh University.

BROWN, F. N. M. (undated) *Stages of boundary layer instability and transition*. Film loop FM-92, Encyclopaedia Britannica Educational Corporation.

BROWN, G. L. & THOMAS, A. S. W. 1977 Large structure in a turbulent boundary layer. *Phys. Fluids Suppl.* **20**, 243.

BRODKEY, R. S. 1978 Flow visualisation and simultaneous anemometry studies of turbulent shear flows. *Workshop on Coherent Structure of Turbulent Boundary Layers*, p. 28. Lehigh University.

CANTWELL, B., COLES, D. & DIMOTAKIS, P. 1978 Structure and entrainment in the plane of symmetry of a turbulent spot. *J. Fluid Mech.* **87**, 641.

CHEN, C. H. P. 1975 The large scale motion in a turbulent boundary layer: a study using temperature contamination. Ph.D. thesis, University of Southern California, Los Angeles.

CHEN, C. H. P. & BLACKWELDER, R. F. 1978 Large-scale motion in a turbulent boundary layer: a study using temperature contamination. *J. Fluid Mech.* **89**, 1.

COLES, D. 1978 A model for flow in the viscous sublayer. *Workshop on Coherent Structure of Turbulent Boundary Layers*, p. 462. Lehigh University.

CORRSIN, S. 1957 *Symposium on Naval Hydrodynamics*. Publ. 515, NAS-NRC, p. 373.

DECKKER, B. E. L. 1980 An investigation of some unsteady boundary layers by the schlieren method. *Int. Symp. on Flow Visualisation*, Ruhr-Universtität. Bochum.

DECKKER, B. E. L. & WEEKES, M. E. 1976 The unsteady boundary layer in a shock tube. *Proc. I. Mech. Eng.* **190** (11), 287.

DINKELACKER, A. 1979 Play tornado-like vortices a role in the generation of flow noise? *IUTAM Symp. on the Mech. of Sound Generation in Flows*, p. 217. Springer.

FALCO, R. E. 1974 Some comments on turbulent boundary layer structure inferred from the movements of a passive contaminant. *A.I.A.A. Paper* 74–99.

FALCO, R. E. 1977 Coherent motions in the outer region of turbulent boundary layers. *Phys. Fluids Suppl.* **20**, 124.

FALCO, R. E. 1978 Combined simultaneous flow visualisation/hot-wire anemometry for the study of turbulent flows. *Non-Steady Fluid Dynamics*, p. 73. A.S.M.E.

FALCO, R. E. & NEWMAN, G. R. 1974 Coherent repetitive Reynolds stress producing motions in a turbulent boundary layer. *Bull. Am. Phys. Soc.* **19**, 1152.

FAVRE, A., GAVIGLIO, J. & DUMAS, R. 1957 Space–time double correlations and spectra in a turbulent boundary layer. *J. Fluid Mech.* **2**, 313.

FIEDLER, H. & HEAD, M. R. 1966 Intermittency measurements in a turbulent boundary layer. *J. Fluid Mech.* **25**, 719.

FRENKIEL, F. N. & KLEBANOFF, P. S. 1973 Probability distributions and correlations in a turbulent boundary layer. *Phys. Fluids* **16**, 725.

HAMA, F. R., LONG, J. D. & HEGARTY, J. C. 1957 On transition from laminar to turbulent flow. *J. App. Phys.* **28**, 388.

HEAD, M. R. & BANDYOPADHYAY, P. 1978 Combined flow visualisation and hot-wire measurements in turbulent boundary layers. *Workshop on Coherent Structure of Turbulent Boundary Layers*, p. 98. Lehigh University.

HEAD, M. R. & BANDYOPADHYAY, P. 1979 Flow visualisation of turbulent boundary layer structure. *AGARD Conf. Proc.* no. 271, p. 25–1.

HEAD, M. R. & BRADSHAW, P. 1971 Zero and negative entrainment in turbulent shear flow. *J. Fluid Mech.* **46**, 385.

HEAD, M. R. & VASANTA RAM, V. 1971 Simplified presentation of Preston tube calibration. *Aero. Quart.* **12**, 295.

HOLDER, D. W. & NORTH, R. J. 1963 *Schlieren Methods*. NPL Notes on Applied Science no. 31. HMSO.

KIM, H. T., KLINE, S. J. & REYNOLDS, W. C. 1971 The production of turbulence near a smooth wall in a turbulent boundary layer. *J. Fluid Mech.* **50**, 133.

KLINE, S. J. 1978 The role of visualisation in the study of the structure of the turbulent boundary layer. *Workshop on Coherent Structure of Turbulent Boundary Layers*, p. 1. Lehigh University.

KLINE, S. J., REYNOLDS, W. C., SCHRAUB, F. A. & RUNSTADLER, P. W. 1967 The structure of turbulent boundary layers. *J. Fluid Mech.* **30**, 741.

KREPLIN, H.-P. & ECKELMANN, H. 1979 Propagation of perturbations in the viscous sublayer and adjacent wall region. *J. Fluid Mech.* **95**, 305.

OFFEN, G. R. & KLINE, S. J. 1973 Experiments on the velocity characteristics of 'bursts' and on the interactions between the inner and outer regions of the turbulent boundary layer. Stanford Univ. Eng. Dept. Rep. MD-31.

PRATURI, A. K. & BRODKEY, R. S. 1979 A stereoscopic visual study of coherent structures in turbulent shear flow. *J. Fluid Mech.* **89**, 251.

SAFFMAN, P. G. 1977 Problems and progress in the theory of turbulence. In *Structure and Mechanisms of Turbulence II* (ed. H. Fiedler), Lecture Notes in Physics, vol. 76, p. 273. Springer.

SMITH, C. R. 1978 Visualisation of turbulent boundary layer structure using a moving hydrogen bubble wire probe. *Workshop on Coherent Structure of Turbulent Boundary Layers*, p. 48. Lehigh University.

THEODORSEN, T. 1952 Mechanism of turbulence. *Proc. 2nd Midwestern Conf. on Fluid Mech.* Ohio State University.

THOMPSON, B. G. J. 1967 A new two-parameter family of mean velocity profiles for incompressible turbulent boundary layers on smooth walls. *Aero. Res. Counc. R. & M.* 3463.

THWAITES, B. 1960 *Incompressible Aerodynamics*. Oxford University Press.

VAN MAANEN, H. R. E. 1979 Experimental study of coherent structures in the turbulent boundary layer of pipe flow using laser-doppler anemometry. *AGARD Conf. Proc.* no. 271, p. 3-1.

WESKE, J. R. & PLANTHOLT, A. H. 1953 Discrete vortex systems in the transition range in fully developed flow in a pipe. *J. Aero. Sci.* **20**, 717.

WILLMARTH, W. W. 1975 Structure of turbulence in boundary layers. *Adv. Appl. Mech.* **15**, 159.

WILLMARTH, W. W. 1978 Survey of multiple sensor measurements and correlations in boundary layers. *Workshop on Coherent Structure of Turbulent Boundary Layers*, p. 130. Lehigh University.